AD_____

Award Number: W81XWH-11-1-0327

TITLE: Inhibition of Embryonic Genes to Control Colorectal Cancer Metastasis

PRINCIPAL INVESTIGATOR: Dr. John Jessup

CONTRACTING ORGANIZATION: The Geneva Foundation, Lakewood, WA 96499

REPORT DATE: September 2012

TYPE OF REPORT: Annual

PREPARED FOR: U.S. Army Medical Research and Materiel Command
Fort Detrick, Maryland 21702-5012

DISTRIBUTION STATEMENT: Approved for public release; distribution unlimited

The views, opinions and/or findings contained in this report are those of the author(s) and should not be construed as an official Department of the Army position, policy or decision unless so designated by other documentation.

REPORT DOCUMENTATION PAGE

Form Approved
OMB No. 0704-0188

Public reporting burden for this collection of information is estimated to average 1 hour per response, including the time for reviewing instructions, searching existing data sources, gathering and maintaining the data needed, and completing and reviewing this collection of information. Send comments regarding this burden estimate or any other aspect of this collection of information, including suggestions for reducing this burden to Department of Defense, Washington Headquarters Services, Directorate for Information Operations and Reports (0704-0188), 1215 Jefferson Davis Highway, Suite 1204, Arlington, VA 22202-4302. Respondents should be aware that notwithstanding any other provision of law, no person shall be subject to any penalty for failing to comply with a collection of information if it does not display a currently valid OMB control number. **PLEASE DO NOT RETURN YOUR FORM TO THE ABOVE ADDRESS.**

1. REPORT DATE *(DD-MM-YYYY)*	2. REPORT TYPE	3. DATES COVERED *(From - To)*
01-09-2012	Annual	1 Sep 2011 - 31 Aug 2012

4. TITLE AND SUBTITLE
Inhibition of Embryonic Genes to Control Colorectal Cancer Metastasis

5a. CONTRACT NUMBER

5b. GRANT NUMBER
W81XWH-11-1-0327

5c. PROGRAM ELEMENT NUMBER

6. AUTHOR(S)
Dr. John Jessup

E-Mail: jessupj@mail.nih.gov

5d. PROJECT NUMBER

5e. TASK NUMBER

5f. WORK UNIT NUMBER

7. PERFORMING ORGANIZATION NAME(S) AND ADDRESS(ES)
The Geneva Foundation
Lakewood, WA 96499

8. PERFORMING ORGANIZATION REPORT NUMBER

9. SPONSORING / MONITORING AGENCY NAME(S) AND ADDRESS(ES)
U.S. Army Medical Research and Materiel Command
Fort Detrick, Maryland 21702-5012

10. SPONSOR/MONITOR'S ACRONYM(S)

11. SPONSOR/MONITOR'S REPORT NUMBER(S)

12. DISTRIBUTION / AVAILABILITY STATEMENT
Approved for Public Release; Distribution Unlimited

13. SUPPLEMENTARY NOTES

14. ABSTRACT

Embryonic core Transcription Factors (TFs), primarily the retrogene NanogP8, are the master regulators of stem cells in human Colorectal Carcinoma (CRC) and positively control neoplastic progression. The major goals of the application are to demonstrate that NanogP8 is expressed in human colorectal carcinoma (CRC) and that inhibition of expression of NanogP8 by lentiviral (LV) short hairpin (shRNA) will regress established human CRC liver xenografts in preclinical models. These data are necessary as proof of principle before we can progress to using LV shRNA in patients with advanced CRC in early phase trials.

15. SUBJECT TERMS
Apoptosis, Lentiviral vector, shRNA, NANOG, NANOGP8, spheroids, xenografts, Colorectal Carcinoma, Caspases, Tissue Microarray

16. SECURITY CLASSIFICATION OF:			17. LIMITATION OF ABSTRACT	18. NUMBER OF PAGES	19a. NAME OF RESPONSIBLE PERSON
a. REPORT	b. ABSTRACT	c. THIS PAGE			USAMRMC
U	U	U	UU	68	19b. TELEPHONE NUMBER *(include area code)*

Table of Contents

Page

Introduction& Hypothesis…….…….…..….. **3 - 4**

Body…….. **4 - 7**

Key Research Accomplishments (TASK Reports) …….. **8**

Reportable Outcomes (TASK Reports, Manuscripts, Abstracts)……. **8**

Conclusion…… **8**

References…… **9**

Appendices…… **2 Appendices**

Appendix I: Zhang et al. Nanog modulates stemness in human colorectal cancer. *Oncogene*. (In Press) 2012. Manuscript plus supplementary data.
Appendix II: Miscellaneous data

Annual Report – First Year of Funding

Hypothesis: Embryonic core transcription factors (TFs), primarily the retrogene NanogP8, are the master regulators of cancer stem cells (CSC) in human colorectal carcinoma (CRC). The corollary is that inhibition of NanogP8 will inhibit neoplastic progression of CRC.

Introduction

During the first year of funding we have not only been successful in two of the three Tasks but also identified new information that establishes the importance of the Nanogs, including NANOGP8, in maintaining the stemness of colorectal carcinoma (CRC) as well as the identification of two different pathways by which NANOG and NANOGP8 control pluripotency in CRC. We will first describe how we have established the importance of NANOGP8 in the maintenance of the stem cell characteristics of CRC and then what we have done to meet the specific aims.

We have submitted a manuscript entitled "NANOG Modulates Stemness in Human Colorectal Cancer" by Zhang et al. (Appendix I) that was just accepted for publication at *Oncogene* that describes the effects of NANOGP8 on stemness of CRC. The findings that were not described in the initial IDEA application are:

- *NANOGP8* is translated into protein in human CRC (Figure 2, Appendix I)
- Expression of *NANOGP8* in CRC with knock down of both *NANOGs* by shNanog rescues stemness as measured by increasing single cell spherogenicity after knock down of both *NANOG*s. The recovery of stemness by *NANOGP8* is stronger than that caused by *NANOG* (Figure 3, Appendix I).
- Our allele-specific shRNA to *NANOGP8* (shNp8-1) delivered by lentiviral vector (LV) inhibits the growth of CRC transduced ex vivo when implanted into NOD/SCID mice to a greater extent than the shRNA to *NANOG* (shNg-1) (Figure 6, Appendix I).
- Inhibition of the *NANOGs* inhibits WEE1 and other kinases associated with the G2/M portion of the cell cycle (Figure 5, Appendix I).
- We have confirmed that NANOG binds Pin-1 (1) an enzyme that stabilizes AKT as a mechanism to promote cell survival (Figure 5, Appendix I) {e.g., inhibition of NANOG protein expression would decrease AKT signaling and enhance apoptosis}.

We have also identified two new pathways by which inhibition of the NANOGs may induce apoptosis in CRC in support of Task 2. RNA-Seq was performed in CX-1 CRC cells transduced either with shNp8-1 to inhibit NANOGP8 or with overexpression of NANOGP8. Those genes that were decreased by shNp8-1 and increased by overexpression of NANOGP8 Gene expression was analyzed by Ingenuity Pathway Analysis identified NEDD9 as an important mediator associated with inhibition of CRC growth (Figure 1, Appendix II). NEDD9 is a scaffolding protein for adhesion plaques that associates c-src kinase with focal adhesion kinase (FAK) to activate FAK by tyrosine phosphorylation (2). We have previously found that FAK appears to be constitutively activated in CRC (unpublished observation) and when activated it provides survival signals through AKT (3). We confirmed that NEDD9 transcripts are regulated by either NANOG because NEDD9 transcripts either decreased when NANOGs are inhibited or increased when NANOGs are overexpressed (Figure 2, Appendix II). NEDD9 overexpression is an anti-apoptotic effector (4) and increases single cell spherogenicity (Figure 3, Appendix II). We have designed a shRNA to NEDD9 (shNEDD9-2) that partially inhibits NEDD9 but it does not entirely decrease NEDD9 protein expression or single cell spherogenicity (Figure 4, Appendix II). We have just obtained a commercial shRNA that is likely to shut down NEDD9 protect expression and if it does we will assess whether inhibition of NEDD9 causes loss of stemness as measured by spherogenicity. We have also performed ChIP and determined that NANOG binds to the NEDD9 promoter as predicted by Boyer et al. (5). Our current hypothesis is that NEDD9 is a mediator by which NANOG mediates stemness. We are currently preparing a manuscript on the role of NEDD9 as a mediator of the effect of NANOG effect on stemness in CRC.

In addition, we postulate a second pathway through which NANOG affects apoptosis. We have previously demonstrated that when CRC cells that normally grow attached to substrates are placed into suspension culture they die over the course of 96 hr through a form of apoptosis termed anoikis (6). The mechanism involves the clustering of TNFRSF10B (TRAIL receptor 2 or DR5) into the death signaling clusters and the activation of caspase 8 and the extrinsic pathway of apoptosis (6). There was essentially no activation of caspase 9 during anoikis which would indicate activation of the mitochondrial or intrinsic pathway of

apoptosis. Since Boyer et al (5) demonstrated that NANOG binds to the Caspase 9 promoter, we postulate that inhibition of either NANOG may activate Caspase 9 and the intrinsic pathway of apoptosis because NANOG acts to repress Caspase 9's promoter. The data accrued under Task 2b suggests that a) Caspase 9 and the intrinsic apoptotic pathway is activated by shRNA to the NANOGs and b) NANOGP8 may act as an activator of NEDD9 but a repressor of Caspase 9.

BODY

Specific Tasks:

Task 1. Confirm that NanogP8 and not Nanog is the important Nanog family member expressed in human CRC (timeframe months 1 -12).

1a. Measure Nanog gene product expression in primary CRC by quantitative immunofluorescence assay (qIFA) (timeframe months 1 – 8)

Nanog and NanogP8 only differ in 2 amino acids so detection of protein with commercial antibodies identifies both gene products. qIFA will be done with SAIC investigator Dr. Kinders in Frederick, MD. The Colon Tissue Microarray (TMA) is available through NCI (http://cdp.nci.nih.gov/colon/progression_tma.html) and contains 367 deidentified primary colon cancers from all stages along with normal colon, adenomas and CRC cell lines as controls and is statistically designed to test the expression of a protein with overall survival and stage of disease by qIFA.

During the first funding period we are analyzing the colon carcinoma TMA that contains 367 primary colon carcinomas along with controls for NANOG and NEDD9 protein expression. This TMA is important because it not only contains information about staging and first course of treatment but also overall survival so that we may assess NANOG as a prognostic factor. We are in the process of measuring NANOG expression by quantitative Immunofluorescence assay (qIFA) and NEDD9 by chromogenic immunohistochemistry (IHC). We include NEDD9 for reasons described above in the **Introduction**. We have found that quantitation of this TMA is difficult because the cases are spread over 8 slides that have different levels of oxidation and hydrolysis. qIFA appears to be useful (Figure 5, Appendix II) because it has the ability to control the dynamic range within each slide and even within individual cores with image analysis software. In contrast, IHC even with image analysis has a smaller dynamic range and the slides are more sensitive to the vagaries of hydrolysis caused by prolonged transport during a heat wave earlier this summer. The results of the coded quantitation of NEDD9 and NANOG levels will be validated after measurement in duplicate, and integrated. My collaborators are Dr. Stephen Hewitt, the director of the Tissue Array Research Program (TARP), Laboratory of Pathology, CCR, NCI and Drs. Scott Lawrence and Robert Kinders of the pharmacodynamics assay development laboratory of SAIC-Frederick and DCTD, Frederick National Cancer Research Laboratory. We anticipate that this will be done by the end of next month and then we will hand the information over to our statistician, Dr. Lisa McShane, who is expected to take another 2 months to complete her analysis because of her workload on other projects. Our statistician has been instrumental in the 'Omics work that the Institute of Medicine is doing in the wake of the Duke genetics fiasco which she helped identify. We will produce a manuscript on the role of the NANOGs and NEDD9 as prognostic markers in colon carcinoma and that will include confirmation of the biologic interaction between NANOG and NEDD9.

1b. Identify the relative transcript expression of Nanog, NanogP8, other family members in CRC by quantitative Reverse Transcriptase-Polymerase Chain reaction (qRT-PCR) and RE Assay (Timeframe months 1-12).

Identification of NanogP8 and the other members of the Nanog gene family requires specific qRT-PCR, our Restriction Endonuclease Assay (RE Assay) and direct sequencing. This will be on up to 20 deidentified primary or metastatic CRC undergoing surgery at NIH through collaboration with Dr. Avital, Surgery Branch, NCI. This subtask will establish the prevalence of NanogP8 expression in clinical tumors. Our data suggest that 70% of clinical mets express NanogP8 transcripts and NanogP8 protein is present in CRC cells.

Our data are included in Appendix 1 and indicates that NANOG protein is expressed in 9 of 10 CRC liver metastases with a NANOG transcript identified in 8 samples and NANOGP8 transcripts present in 6 of the 8 samples and the only transcript in 2. This indicates that NANOGP8 transcripts are frequently expressed in CRC. We have not found the expression of other NANOG pseudogenes in clinical samples with only 1 instance each of NANOGP4 and NANOGP7.

For Milestone 1: While we do not have final analysis yet on the TMA, it is clear from the early data that NANOG protein is expressed in more than 40% of colon carcinomas analyzed so far.

Task 2a. Determine whether inhibition of NanogP8 or other embryonic TFs by LV shRNA inhibits cell proliferation in CRC in vitro (Timeframe Months 6 -12)

We have focused only on NANOG because inhibition of NANOGs inhibits OCT4 and to a lesser extent SOX2 (Appendix 1).

We analyzed whether proliferation was inhibited by allele-specific shRNA to NANOGP8. We confirmed this with the WST1 assay (Figure 6, Appendix II). shRNA to NANOGP8 (shNp8-1) was more active in inhibiting proliferation as measured by WST1 assay. We also demonstrated that over-expression of NANOGP8 increased proliferation in all 3 cell lines. This completes the analysis of this task and confirms that inhibition of NANOGP8 by shNp8-1 is more active against the CRC lines than inhibition of NANOG alone by shNg-1.

Task 2b. Establish whether transduction of shRNA targeting NanogP8 induces apoptosis in CRC lines (Timeframe Months 6 -24)

We first assessed whether LV shRNA transduction decreased the size of 3-D aggregates and spheroids of CRC. CRC cells stably expressing LUC2 were cultured under Ultra Low Attachment (ULLA) conditions for 24 hours to form multicellular aggregates and spheroids. Then these 3-D cultures were exposed to LV shRNA (Figure 7a, Appendix II). Cultures were analyzed 72 hours later for tumor growth by optical microscopy and luminescence. CX-1 transduced with LV shNp8-1 (shRNA to NANOGP8) were ~50% smaller than either untreated CX-1 cells or CX-1 cells transduced with LV shNeg, the negative control vector (Figures 7b, c, Appendix II). CRC cultures transduced with LV shNg-1 (shRNA to NANOG) were smaller than those transduced with shNeg, the negative control vector, but not as small as cells transduced with shNp8-1 (Figures 7b, c, Appendix II). Optical measurements of tumor area correlated with luminescence of the tumor cells 72 hr after LV transduction with Spearman correlation coefficient and two-tailed P values of Rs= 0.78 with P=0.0064 for CX-1 (Figure 7d, Appendix II) and Rs=0.86 with P=0.01 for Clone A (Figure 7e, Appendix II). Subsequent measurements of tumor area after LV transduction were made optically and indicated that LV shNp8-1 decreased tumor area by 33 – 45% in 72 hr (Figure 7f, Appendix II). Since overexpression of NANOG or NANOGP8 stimulated tumor growth (Figure 7f, Appendix II), the reduction in tumor growth by shRNA to either NANOG gene was due to inhibition of the gene and not off target effects. Furthermore, when surviving tumor cells were replated in serum-containing medium in monolayer cultures for 11 – 14 days, plating efficiency was decreased by 15% in Clone A cells and 44% in CX-1 cells (Figure 7g – h, Appendix II). Thus, transduction with LV shNp8-1 inhibited 3-D growth of CRC and decreased their replating efficiency.

We then assessed whether LV inhibition of NANOG or NANOGP8 induced apoptosis in CRC. Spheroids were transduced with LV shRNA as described in Figure 7, Appendix II and then analyzed by single cell profiling with fluorescent peptides that become fluorescent when cleaved by an active caspase. An example of assessment by inverted microscope (Figure 8 a-d, Appendix II) or confocal microscopy (Figure 8e-g, Appendix II) are presented along with a measurement of transduction efficiencies in Clone A, CX-1 and LS 174T cells for the various shRNA constructs. The transduction efficiencies ranged from just under 40% to nearly 80% (Figure 8h, Appendix II). When CRC were exposed to LV shNg-1, shNp8-1 or the control shNeg for 3 days and then analyzed for Annexin V staining, LV shRNA to either NANOG gene had a minimal effect on Annexin V staining when Clone A, CX-1 or LS 174T cells were cultured in monolayer (Figures 9 a, c, e, Appendix II). However, culture in suspension increased Annexin V staining in all 3 cell lines by at least three-fold over that of those cells in monolayer (Figures 9a, c, e, Appendix II) and is consistent with our prior findings (6). Transduction with LV shNp8-1 further increased Annexin V expression significantly in Clone A and CX-1 but not LS 174T (Figures 9a, c, e, Appendix II). Thus, LV shRNA does not increase Annexin V staining in monolayer. However, inhibiting NANOGP8 in suspension culture increased Annexin V staining compared to the untreated CRC cells in Clone A or CX-1 but not LS 174T.

When cells were transduced after 24 hr of suspension culture and then assessed for caspase 8, 9 or 3 activity in a single cell profiling assay, CRC cells with caspase 3 and 9 activity were significantly increased by LV shNp8-1 transduction (35 – 45%) compared to the 10 – 20% of untreated cells in suspension (Figure 9b, d, f, Appendix II). Caspase 8 activity was increased in untreated CX-1 and LS 174T cells in suspension without

further increase by transduction with shNp8-1 while caspase 8 activity was increased in Clone A by transduction with LV shNp8-1. Transduction with the shRNA to NANOG (shNg-1) increased caspase activity in these lines but to a lesser extent than transduction with shNp8-1 (Figure 9b, d, f, Appendix II). To confirm that the intrinsic pathway was more important than the extrinsic pathway in CRC transduced with LV shNp8-1 we assessed whether peptide inhibitors that block caspase 8, 9 or 3 inhibited the activity of the LV shRNAs. Inhibitors of caspase 3 and 9 blocked apoptosis in CRC lines when 10 μM was included in the culture medium shortly after exposure of CRC to lentivirus (Figure 10, Appendix II). Treatment with 10 μM caspase 8 peptide inhibitor failed to block anoikis in Clone A and CX-1 but inhibited anoikis in LS 174T cells (Data Not Shown). Thus, lentiviral shRNA to NANOGP8 more than NANOG induces apoptosis in three-dimensional suspension culture of CRC lines. These results complement those obtained with the NEDD9 and suggest that the inhibition of NANOG and NANOGP8 might enhance caspase 9 activity. Since Boyer et al (5) demonstrated that NANOG binds to the caspase 9 promoter as well as the NEDD9 promoter, we are assessing whether NANOG may function as a repressor of caspase 9 while being an activator of NEDD9 and will test the effect of NANOG expression on a commercially available caspase 9 promoter reporter. NANOG has been considered to be both a promoter activator and repressor for other genes so it is possible that NANOG may directly alter caspase 9 expression to activate the intrinsic pathway of apoptosis. As a result, during the first year of the grant we have identified two different pathways that activate apoptosis and are developing the tools to confirm this as well as to write the manuscripts that support these findings.

Task 2 Milestones: A. Determine the MOI to cause 50% inhibition of NanogP8 in CX-1 and LS 174T cells that stably express LUC2. Our MOI for inhibition of proliferation as measured by WST1 is an MOI 0f 10:1. **B. Determine whether inhibition of NanogP8 gene expression by at least 50% compared to untreated parental cell line causes either inhibition of cell proliferation or induction of apoptosis in 3 of 6 CRC lines in monolayer cultures**. We have shown that LV-delivered shNp8-1 inhibits tumor growth by 50% at a MOI of 5 in 3 CRC lines, including the 2 to be used in Task 3.

Task 3a. Determine the efficacy of intralesional injection of lentivirus shRNA to NanogP8 or other embryonic genes on CRC tumors in the livers of NOD/SCID mice (Timeframe Months 6 – 24).

There were three phases to this aim in the IDEA application. First phase was to assess the ability of intralesional therapy to transduce established nodules of CRC in vivo in the sub cutis to inhibit tumor growth. The second phase was to transduce small nodules of tumor growing in the liver while the third phase was to determine whether systemically delivered lentiviral shRNA could inhibit tumor growth in the liver and abdomen. We reached an obstacle in the first phase. When we injected ~3mm diameter subcutaneous nodules with 0.10 ml of PBS intralesionally containing ~5 x 10^6 lentiviral particles of shNg-1, shNp8-1 or the control shNeg we achieved modest but not significant reduction in size of nodules. However, the negative control provided essentially as great a reduction as the anti-NANOGs shRNA (Figure 11, Appendix II). This suggested that the immune response to the lentivirus itself was causing a nonspecific inhibition of tumor growth. This was confirmed when we tried on several occasions to then determine whether transduction of tumor cells within the nodules occurred. We developed a rapid isolation technique to create a single cell suspension and then evaluated GFP fluorescence under an inverted microscope. Since our lentiviral shRNA constructs all express Green Fluorescent Protein (GFP) as a reporter, the tumor cells should express GFP if they are transduced. However, as can be seen in the attached figure, they do not (Figure 12, Appendix II) – especially when compared to cells within a spheroid transduced in vitro that clearly express functional GFP (Figure 8, Appendix II). Examination of the literature as well as the recent American Society of Gene Therapy meeting indicates that intralesional therapy with shRNA is not an especially active area of investigation in cancer therapeutics, possibly because of this lack of transduction in vivo.

We are pursuing four approaches to overcome this obstacle that will move intratumoral gene therapy forward if successful:

Approach 1: Increase the multiplicity of infection (MOI). Our most obvious problem is that we may not have delivered enough lentivirus vector to the tumor since we transduced at what in retrospect was at a MOI of 1 whereas a MOI of at least 5 was used to decrease tumor growth in vitro. To pursue this, we have formed a collaboration with Dr. Jakob Reiser of the Center for Biologics Evaluation and Research, FDA who is a Senior Staff Fellow and Principal Investigator in OCTGT / DCGT / GTIB and an international expert on selective

targeting of lentivirus. Xenografts with an average diameter of 15μ (e.g., Clone A) in 4 - 6 mm diameter nodules have ~ 10^6 cells that then require 5 – 10 x 10^6 LV particles to achieve a Multiplicity of Infection (MOI) of 5. The Reiser lab has produced batches of research-grade LV at titers up 10^{10} transducing units/ml or above (7, 8) that support MOIs of 5 – 10. 5 mm CX-1 tumors will be injected at varying MOI, harvested at 5 days and analyzed for transduction by GFP fluorescence and qPCR analysis. He is developing our lentiviral constructs in large high grade research batches for testing intralesional therapy at higher concentration and MOI. This is the most obvious and direct way to approach this problem. We anticipate that the first batches will be prepared by the end of August and certified by his lab for use.

Approach 2: Develop an improved selective targeting vector. We are developing a single-chain variable fragment (scFv)-based LV to increase the selective binding to tumor cells which may be greater than that of the standard VSV-G pseudotyped LV particle (9). The scFv (10) binds to Carcinoembryonic Antigen (CEA) which is expressed not only on colorectal carcinoma (CRC) but essentially all carcinomas and has been graciously provided by Dr. J. Shively at the City of Hope National Cancer Center. As depicted below, this scFv is linked through a G_4 linker to membrane anchors (the GPI-membrane anchor of CEA itself or the VSV-G-derived transmembrane/fusion domain (VSV-GS) provided by Dr. Reiser, Figure 2). VSV-GS has a truncated extracellular domain so it lacks binding to the native receptor(s) on cells while retaining the fusogen that supports viral membrane fusion with target cell membranes (11, 12). The Reiser lab will oversee production of virus as well as evaluate transduction efficiency and other aspects of quality control while the Jessup lab will test binding specificity on CEA + (CX-1) and CEA – (Clone A) CRC lines. The scFv vector with the best transduction efficiency and specificity for CEA+ CRC will be used for in vivo transduction analysis.

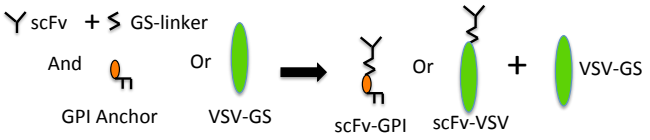

Figure 13. Schematic of scFV targeting vectors. ***Anti****-CEA scFv combined with G_4 linker and bound to either the CEA GPI linker or the VSV-G-derived transmembrane domain. Each of these constructs will be paired with VSV-GS domain to pseudotype LV particles encoding the shRNA and a GFP reporter.*

Approach 3. Determine whether host stroma or alterations in pH or serum are a barrier to transduction. For this aim we will use our in vitro 3-D system (Figure 7, Appendix II) to test whether murine fibroblasts inhibit LV transduction of CRC cells. VSV-G pseudotyped LV shNG-1 or shNp8-1 inhibit growth in suspension of established aggregates/spheroids in serum free medium in ultra low attachment (ULLA) plates (Figure 7). Transduction of murine 3T3 cells by VSV-G-pseudotyped LV is low. We will co-culture 3T3 cells with human CRC in various ratios in our 3-D assay and then determine whether their presence inhibits transduction of CRC significantly with either the standard VSV-G pseudotype or the scFv-displaying LV vectors. Alterations in pH and mouse serum will also be tested in this in vitro co-culture system since both pH (13) and serum with complement (14) may alter viral transduction and targeting. Our LV shRNA vectors contain a GFP reporter that will be used to monitor transduction. We will also use the far red lipid fluorophore DID (15) to label LV membranes so that confocal microscopy can monitor whether LV bind to target cells, can fuse and then whether transduction occurs by assessing fluorescence dequenching of DID (16).

Approach 4: Determine whether interstitial pressure within the xenograft inhibits viral:carcinoma cell receptor-ligand binding and/or subsequent membrane fusion, or endosomal release, reverse transcription, nuclear uptake and integration since interstitial pressure within tumors inhibits uptake of large molecules or particles (17). This will be assessed in vivo by using DID-labeled LV shRNA particles injected into 5 mm CEA-expressing (CX-1 and LS 174T) and CEA negative (Clone A) CRC xenografts growing subcutaneously. Samples will be collected at defined times after intralesional injection over 5 days and analyzed by confocal microscopy and single cell analysis for binding to CRC, internalization after membrane fusion and expression of GFP, and by qPCR to monitor reverse transcription, nuclear uptake, and integration (18).

Key Research Accomplishments

- Established that NANOGP8 can rescue stemness in CRC cells
- Established that LV shRNA can transduce 3-D spheroids with good efficiency
- Established that inhibition of NANOGP8 and to a lesser extent NANOG induces apoptosis through the intrinsic pathway
- Identified that NANOG and/or NANOGP8 may activate NEDD9 and possibly repress Caspase 9 as mechanisms for inducing apoptosis – two separate possible pathways that stimulate apoptosis
- Found difficulty in transducing CRC xenografts in vivo in NOD/SCID mice

Reportable Outcomes

Manuscript (In Press)

1. Zhang J, Espinoza LA, Kinders RJ, Lawrence SM, Pfister TD, Zhou M, Veenstra T, Tang DG, Jeter C, Thorgeirsson SS, Jessup JM. Nanog modulates stemness in human colorectal cancer. *Oncogene*. (accepted for publication 8/17/12) 2012.

Abstracts with presentations in 2012

1. Zhang J, Thorgeirsson SS, Jessup JM. Allele-Specific Inhibition Of Nanog Family Members Inhibits Three-Dimensional (3-D) Growth Of Human Colorectal Carcinoma (CRC) In Vitro. Presented at the Annual Meeting of the American Society of Gene and Cell Therapy, Philadelphia, PA March 2012.
2. Zhang J, Thorgeirsson SS, Jessup JM. Allele-specific shRNA to Nanog family members inhibits 3-D growth of colorectal carcinoma through the intrinsic apoptotic pathway. In: *Proceedings of the 103rd Annual Meeting of the American Association for Cancer Research*; 2012 Mar 31-Apr 4; Chicago, Illinois. Philadelphia (PA): AACR; 2012. 5646

These abstracts as well as the manuscript have been submitted to Geneva Research Foundation.

Conclusion

In summary, we have completed TASKs 1b and 2 and will in the next 4 months complete TASK 1a. During this first year of the grant, we have demonstrated that NANOGP8 can rescue stemness in CRC when expression of both NANOG genes is inhibited. This IDEA grant has also developed new insights into how NANOG, and more importantly the retrogene NANOGP8, maintains pluripotency in CRC by acting as a positive activator of NEDD9 and possibly as a repressor of Caspase 9. These results are critical because they support the further development of therapeutics that target NANOGP8 and perhaps NANOG as a means to inhibit cancer growth and progression.

References

1. Nishi M, Akutsu H, Masui S, Kondo A, Nagashima Y, Kimura H et al. A distinct role for Pin1 in the induction and maintenance of pluripotency. J Biol Chem 286: 11593-11603, 2011.
2. Izumchenko E, Singh MK, Plotnikova OV, et al. NEDD9 promotes oncogenic signaling in mammary tumor development. Cancer Res. 69:7198-206, 2009.
3. Beauséjour M, Noël D, Thibodeau S, et al. Integrin/Fak/Src-mediated regulation of cell survival and anoikis in human intestinal epithelial crypt cells: selective engagement and roles of PI3-K isoform complexes. Apoptosis 17:566-78, 2012.
4. Singh M, Cowell L, Seo S, O'Neill G, Golemis E. Molecular basis for HEF1/NEDD9/Cas-L action as a multifunctional co-ordinator of invasion, apoptosis and cell cycle. Cell Biochem Biophys. 48:54-72, 2007.
5. Boyer LA, Lee TI, Cole MF, et al. Core transcriptional regulatory circuitry in human embryonic stem cells. Cell. 122:947-56, 2005.
6. Laguinge LM, Samara RN, Wang W, El-Deiry WS, et al. DR5 receptor mediates anoikis in human colorectal carcinoma cell lines. Cancer Res. 68:909-17, 2008.
7. Kutner RH, Zhang XY, Reiser J. Production, concentration and titration of pseudotyped HIV-1-based lentiviral vectors. Nature Protocols 4:495-505, 2009.
8. Kutner RH, Puthli S, Marino MP, Reiser J. Simplified production and concentration of HIV-1-based lentiviral vectors using HYPERFlask vessels and anion exchange membrane chromatography. BMC Biotechnol. 16;9:10, 2009.
9. Cronin J, Zhang XY, Reiser J. Altering the tropism of lentiviral vectors through pseudotyping. Curr Gene Ther. 5:387-98, 2005.
10. Wu AM, Chen W, Raubitschek A, Williams LE, Neumaier M, Fischer R, Hu SZ, Odom-Maryon T, Wong JY, Shively JE. Tumor localization of anti-CEA single-chain Fvs: improved targeting by non-covalent dimers. Immunotechnology 2:21-36,1996.
11. Zhang XY, R. Kutner R, Bialkowska A, Klimstra WB, Reiser J. Cell-specific targeting of lentiviral vectors mediated by fusion proteins derived from Sindbis virus, vesicular stomatitis virus, or avian sarcoma/leukosis virus. Retrovirology 2010, 7:3, 2010.
12. Goyvaerts C, De Groeve K, Dingemans J, et al. Development of the Nanobody display technology to target lentiviral vectors to antigen-presenting cells. Gene Ther. 2012 Jan 12. [Epub ahead of print].
13. Morizono K, Chen IS. Receptors and tropisms of envelope viruses. Curr Opin Virol. 1:13-18, 2011.
14. DePolo NJ, Reed JD, Sheridan PL, Townsend K, Sauter SL, Jolly DJ, Dubensky TW Jr. VSV-G pseudotyped lentiviral vector particles produced in human cells are inactivated by human serum. Mol Ther. 2:218-22, 2000.
15. Ayala-Nuñez NV, Wilschut J, Smit JM. Monitoring virus entry into living cells using DiD-labeled dengue virus particles. Methods. 2011 Oct;55(2):137-43. Epub 2011 Aug 10.
16. Rust MJ, Lakadamyali M, Brandenburg B, Zhuang X. Single-virus tracking in live cells. Cold Spring Harb Protoc. 2011(9). pii: pdb.top065623.
17. Hagendoorn J, Tong R, Fukumura D, Lin Q, Lobo J, Padera TP, Xu L, Kucherlapati R, Jain RK. Onset of abnormal blood and lymphatic vessel function and interstitial hypertension in early stages of carcinogenesis. Cancer Res. 66:3360-4, 2006.
18. Mbisa JL, Delviks-Frankenberry KA, Thomas JA, Gorelick RJ, Pathak VK. Real-time PCR analysis of HIV-1 replication post-entry events. Methods Mol Biol. 485:55-72, 2009.

Appendix I

NANOG Modulates Stemness in Human Colorectal Cancer

Jingyu Zhang[1]*, Luis A. Espinoza[1]*, Robert J. Kinders[2], Scott M. Lawrence[2], Thomas D. Pfister[2], Ming Zhou[3], Timothy D. Veenstra[3], Snorri S. Thorgeirsson[1], J. Milburn Jessup[1,4,5]

*These authors contributed equally to this work

[1]Laboratory of Experimental Carcinogenesis, National Cancer Institute, Center for Cancer Research, National Institutes of Health, 37 Convent Drive, Bethesda MD 20892

[2]Laboratory of Human Toxicology and Pharmacology, Applied/ Developmental Research Support Directorate, SAIC-Frederick, Inc., NCI-Frederick, Frederick MD 21702

[3] Laboratory of Proteomics and Analytical Technologies, SAIC-Frederick, NCI-Frederick, Frederick MD 21702

[4]Cancer Diagnosis Program, Division of Cancer Treatment and Diagnosis, 6130 Executive Boulevard, Rockville, MD 20852

[5]To whom correspondence should be directed: J. M. Jessup, MD, Chief, Diagnostics Evaluation Branch, Cancer Diagnosis Program, Rockville MD 20892-7420; Office: 301-435-9010; Fax: 301-402-7819.

Running Title: NANOGP8 modulates stemness in CRC

6 Figures with 3 in color

Total Words excluding Abstract, References and Figure Legends – 4,443

Abstract

NANOG is a stem cell transcription factor that is essential for embryonic development, reprogramming normal adult cells and malignant transformation and progression. The nearly identical retrogene NANOGP8 is expressed in multiple cancers, but generally not in normal tissues and its function is not well defined. Our postulate is that NANOGP8 directly modulates the stemness of individual human colorectal carcinoma (CRC) cells. Stemness was measured in vitro as the spherogenicity of single CRC cells in serum free medium and the size of the side population and in vivo as tumorigenicity and experimental metastatic potential in NOD/SCID mice. We found that 80% of clinical liver metastases express a *NANOG* with 75% of the positive metastases containing *NANOGP8* transcripts. 3 to 62% of single cells within 6 CRC lines form spheroids in serum free medium in suspension. *NANOGP8* is translated into protein. The relative expression of a *NANOG* gene increased 8-122 fold during spheroid formation, more than the increase in *OCT4* or *SOX2* transcripts with *NANOGP8* the more prevalent family member. shRNA to *NANOG* not only inhibits spherogenicity but also reduces expression of *OCT4* and *SOX2,* the size of the side population and tumor growth in vivo. Inhibition of *NANOG* gene expression is associated with inhibition of proliferation and decreased phosphorylation of G2-related cell cycle proteins. Overexpression of NANOGP8 rescues single cell spherogenicity when *NANOG* gene expression is inhibited and increases the side population in CRC. Thus, NANOGP8 can substitute for NANOG in directly promoting stemness in CRC.

Keywords: NANOG; NANOGP8; stemness; colorectal cancer; cancer stem cell

Word count - 245

Introduction

Normal and malignant adult cells retain the capacity to be reprogrammed to induced pluripotent stem cells (iPS) cells from mouse and human adult cells (1-3), from patients (4) and from cancer cells (5). The core embryonic stem cell (ES) transcription factors (TFs) OCT4, SOX2 and NANOG are central to such reprogramming although other genes like KLF4, c-Myc, Lin28 (1-3) are also involved. NANOG is essential for stemness in adult cells (6) and during embryonic development (7,8), while OCT4 and SOX2 are dispensable for reprogramming iPS cells (9, 10). NANOG is a homeobox protein that is regulated at the allelic level to maintain the pluripotent ground state (11). *NANOG* has a retrogene *NANOGP8* that appears to be the prevalent *NANOG* expressed in human breast cancer (12), prostate cancer (13, 14), medulloblastoma and glioblastoma multiforme (15, 16), colorectal carcinoma (13, 17 - 20) and leukemia (21). Inhibition of *NANOG* expression has led to a reduction in tumorigenicity and such in vitro characteristics of stem cells as anchorage independent growth (13, 19) whereas overexpression may increase tumorigenicity (14). The role of *NANOGP8* as a potential substitute for *NANOG* when *NANOG* is absent is not entirely clear. Jeter et al., (13) demonstrated that overexpression of *NANOGP8* in cells transfected with a Lentiviral vector encoding shRNA targeting *NANOG*'s 3'UTR 'rescued' proliferation but not in cells transfected with shRNA targeting the coding sequence of *NANOG*. Thus, the role of NANOGP8 in maintaining the stemness of malignant cells needs further definition.

Our purpose in this study was to define whether *NANOGP8* could replace *NANOG* in CRC in mediating stem cell like characteristics. We assessed this by assessing the ability of *NANOGP8* to 'rescue' spherogenicity in individual CRC cells whose *NANOG* expression had been inhibited. During this study, we confirmed and extended the observations of others (13, 17-20) that both *NANOG* and *NANOGP8* are expressed in clinical metastases of CRC, that inhibition of NANOG reduces the expression and activity of several regulators of G2 cell cycle progression and that inhibition of *NANOGP8* decreases the stem-like activities of CRC both in vitro and in vivo. Finally, we show that the capacity of individual CRC cells to form spheroids in suspension culture in serum free medium can be maintained by *NANOGP8* in the absence of *NANOG*.

Results

The Retrogene *NANOGP8* is Upregulated in Clinical Samples

NANOG and its retrogene *NANOGP8* (12, 13, 16) are frequently upregulated in human cancers. To investigate if *NANOG* is expressed in CRC, we first did an immunofluorescent assay (IFA) on ten clinical liver metastases with a commercially available NANOG antibody, which recognizes both NANOG and NANOGP8. NANOG was mainly located in cytoplasm in CRC (Figure 1a) as described by Meng *et al* (18). This is in contrast to the control specimen of a human seminoma – a germ cell tumor – that has the expected intranuclear location for NANOG (Figure 1b). CD44v6 was used to mark CRC cells because its expression reflects propensity for metastasis in CRC patients (22). When the antibody to NANOG was blocked with recombinant NANOG peptides, the fluorescence due to NANOG was removed (Supplementary Figures 1a-e). The IFA staining is specific to NANOG and eight of ten liver metastases express NANOG proteins (Supplementary Table 1).

In order to further distinguish which *NANOG* is expressed in clinical samples, we examined the transcripts for those genes. Since *NANOGP8* is an intronless retrogene located on chromosome 15 whereas the *NANOG* gene is located on chromosome 12 (23) and differs by 6 nucleotides with one (12) or 2 to 3 non-synonymous amino acid changes due to other nonconserved nucleotide changes (13, 16, 24), we found a single restriction endonuclease that distinguishes the two genes: AlwNI (25), an enzyme that identifies a palindromic hexanucleotide sequence in *NANOGP8* but not in *NANOG* at position 144 relative to the translational start site (Figure 1c). *NANOG* transcripts were identified in 8 of 10 liver metastases and also in 4 adjacent microscopically normal liver sections (Figures 1d-f). Moreover, 6 of the 8 positive tumor specimens contained *NANOGP8* transcripts with 2 each containing only *NANOGP8* or *NANOG* transcripts. Only one of the adjacent liver specimens contained *NANOGP8* while the 3 others only expressed *NANOG* transcripts (Figure 1d-f). Sanger sequencing confirmed the endonuclease results (data not shown). Thus, based on this small sample approximately 80% of clinical CRC metastases expressed *NANOG* family members with 75% of those expressing *NANOGP8*.

The Retrogene *NANOGP8* is the Prevalent *NANOG* expressed in CRC

Expression of *NANOGP8* in clinical tissues is important but is it translated and functional in CRC? To assess this, we investigated whether ES TFs and other CSC related markers are upregulated in 6 CRC lines during formation of spheroids in serum free medium. Relative expression of *NANOG* transcripts was consistently increased in spheroids 8 – 122-fold compared to monolayer cultures except in KM12c whereas the relative expression of *OCT4* was ~40-fold. The *SOX2* expression varied between 1 and 63-fold in spheroids compared to monolayer cultures (Figures 2a and b). However, the expression of CD44, CD133 or CD166 was not significantly increased in spheroid cultures compared to monolayer except in KM 12c, CX-1 and LS 174T (Supplementary Figures 2a and b). When cDNA from the CRC lines was digested with AlwNI, *NANOGP8* was expressed in both the monolayer (Figure 2c) and spheroid cultures (Figure 2d) of the 6 CRC lines. Over 84% of the *NANOG* expressed in monolayer cultures of CX-1 and Clone A was *NANOGP8* and this expression increased to over 94% in spheroids (Figure 2e). The results were confirmed by direct sequencing (data not shown). Thus, expression of *NANOG* transcripts is increased as CRC transition to vertical growth to form spheroids, *NANOGP8* is the prevalent form of *NANOG* expressed in CRC cell lines and was the most consistently up-regulated TF in this panel of 6 CRC lines compared to *OCT4* and *SOX2*.

To confirm that *NANOGP8* is translated in CRC, we used tandem mass spectrometry (MS/MS) to identify the NANOGP8 protein in CRC lines. Extracts from Clone A overexpressing NANOGP8 were immunoprecipitated, isolated by SDS-PAGE, subjected to in gel tryptic digestion followed by MS/MS. Four NANOG-related peptides (KTWFQNQRM, KYLSLQQMQELSNILNLSYKQ, KKEDKVPVKK, and KGKQPTSAENSVAKK) were identified in extracts from Clone A overexpressing NANOGP8. Interestingly, the last peptide is unique to NANOGP8, with the shift from Lys (K) in NANOG to Asn (N) in NANOGP8 at codon 82 (Figure 2f and Supplementary Figure 3a). This amino acid change was also reported (16, 24) and confirmed by gene sequencing. NANOG/NANOGP8 proteins were not identified in extracts of CRC cell lines without overexpression by transduction presumably because CRC cell lines express low levels of endogenous proteins.

Modulation of *NANOG* Gene Expression Affects Spherogenicity of Individual CRC Cells

The capacity of single CRC cells to form spheres – a hallmark of malignant potential – was tested in 6 cell lines in serum-free medium in ultra-low attachment (ULLA) plates in individual wells with spheroids of 50 or more cells scored after at least 9 days of culture. All CRC lines formed spheroids at frequencies that ranged from 1 – 56% of single cells plated (Figure 3a).

We then inhibited total *NANOG* mRNA expression using lentiviral-delivered shRNA to examine the functional relevance of NANOG in spherogenicity in CRC cell lines. Transduction of Clone A and CX-1 with a commercial shNanog reduced *NANOG* transcript levels in Clone A and CX-1 by at least 50% (Supplementary Figures 4c and d) and NANOG protein levels by 90% (Figure 3b). In addition, shNanog transduction decreased *OCT4* transcripts significantly in both Clone A and CX-1 with trends in reduction of *SOX2* transcript levels (Supplementary Figures 4a and b). Interestingly, overexpression of *NANOG* and *NANOGP8* increased *NANOG* transcripts in shNanog transductants by at least two-fold over the untreated parental cells (Supplementary Figures 4c and d) with only the overexpressed *NANOG* or *NANOGP8* transcripts in each line (Figures 3e and f). shNanog transduction alone significantly decreased formation of spheres in both Clone A and CX-1 by 40% - 90% compared to untreated parental cells and cells transduced with the empty vector pLKO.1 (Figures 3c and d). Moreover, shNanog transductants of Clone A and CX-1 lacked expression of *NANOG* but did express *NANOGP8*, albeit at reduced levels (Figures 3e and f, respectively). When Clone A shNanog cells were secondarily transduced with *NANOG* or *NANOGP8*, the level of NANOG transcripts were a fold higher while the *NANOGP8* levels were increased by nearly 30% compared to levels in shNanog Clone A (Figure 3e). When the relative distribution of *NANOG* and *NANOGP8* is combined with the increase in levels of transcripts in the shNanog cells overexpressing *NANOG* or *NANOGP8* the levels of either gene were similar to those of the parental untreated Clone A or CX-1 (Figures 3c and d, Supplementary Figures 4 c and d). Overexpression of *NANOGP8* significantly increased spherogenicity in both Clone A and CX-1 shNanog cells but overexpression with *NANOG* only increased spherogenicity in Clone A shNanog (Figures 3c and d). The inability of *NANOG* overexpression to 'rescue' spherogenicity in CX-1 may be associated with the response of the

CX-1 cells to transduction with *NANOG* since the relative gene transcript expression is not as high as in Clone A even though the total *NANOG* transcript levels were higher in the overexpressing shNanog cells than in the parental untreated cells (Supplementary Figures 4 c and d). In contrast, transduction with *NANOGP8* did achieve similar relative increases over the transcript levels in shNanog transductants. Thus, *NANOGP8* expression appears to rescue the capacity of single CRC cells to form spheroids in the absence of parental NANOG.

Inhibition of NANOG Decreases Tumorigenicity and Experimental Metastasis by CX-1

CRC were injected subcutaneously in NOD/SCID mice in cell dilutions of 10^3 – 10^5 cells per mouse. At 10^3 and 10^4 cells per mouse CX-1 cells transduced with shNanog had fewer tumors than did either the parental cell line or the pLKO.1 control (Figure 4a). We elected to test different constructs in NOD/SCID mice injected subcutaneously with 10^5 cells in order to assess tumorigenicity at a consistent cell concentration between experiments. The growth of shNanog transduced CX-1 was slower than the pLKO.1 control since the median number of days to palpable tumor is increased about 50% (Figure 4b). However, overexpression of either *NANOG* or *NANOGP8* can dramatically shorten the time to palpable tumor (Figure 4b). In addition, 50% of the mice in the shNanog CX-1 groups remained tumor free during the time of the experiment (Figure 4b). Thus, inhibition of NANOG decreased the growth of CX-1 in vivo.

Another test of the effect of shRNA to *NANOG* on the malignant phenotype involves experimental metastasis since liver colonization after intrasplenic injection of viable CRC cells is associated with recurrence in patients operated on for cure (26). shNanog CX-1 cells failed to form grossly visible or microscopic hepatic liver colonies compared to either the parental CX-1 cells or CX-1 cells transduced pLKO.1 (Figure 4c).

Mechanism of Action of Inhibition of *NANOG*

Transductants of CX-1 and Clone A were analyzed for the effect of *NANOG* inhibition or overexpression on cell proliferation. Analysis of cell proliferation indicated that shRNA of *NANOG* caused both CX-1 and Clone A cells to proliferate more slowly than the parental or empty vector control (Figures 5a and b). In contrast, *NANOG* or *NANOGP8* overexpression in

Clone A or NANOG in CX-1 increased cell proliferation (Figures 5a and b). When cell cycle protein expression was analyzed, Wee1 expression (Figure 5c) was decreased significantly with down regulation of phosphorylation of Cdc2, Cdc25C and other proteins involved in the G2/M aspect of the cell cycle (Figure 5c). To further explore the potential molecular mechanisms of *NANOG*-promoted cell proliferation in CRC, we analyzed the interaction between NANOG and Pin 1, a mitotic kinase that is phosphorylated on multiple Ser/Thr-Pro motifs (27) to maintain pluripotency and cell proliferation (28). IFA results show both NANOG and Pin 1 are perinuclear in Clone A (Figure 5d). Reciprocal co-immunoprecipitation experiments confirmed that NANOG and Pin 1 interact in Clone A and Clone A transduced NANOGP8 (Figure 5e). Thus, NANOG proteins may have a cytoplasmic function as well as its function as a transcription factor.

Inhibition of *NANOGP8* Decreases Spherogenicity, Inhibits tumorigenicity and Affects Side Population

If *NANOGP8* is the prevalent form of *NANOG* expressed in CRC, then it would be appropriate to target *NANOGP8* to spare inhibition of *NANOG* if it is required for normal adult stem cell function. shRNAs were designed for both *NANOG* and *NANOGP8* based on guidelines developed for inhibition of single nucleotide polymorphisms (SNPs) (29, 30). The designs are termed allele-specific shRNA to *NANOG* because, although not alleles at the same locus, the single nucleotide differences between *NANOG* and *NANOGP8* are similar to targeting SNPs. shRNAs were designed to target the most 3' single nucleotide difference at nucleotide 759 in the coding sequence (Supplementary Figure 3b). When tested for specificity of inhibition of *NANOG* versus *NANOGP8*, the shRNAs were tested on the human embryonal carcinoma PA-1 that only expresses *NANOG* (12) which is confirmed by AlwNI cutting and direct sequencing (Supplementary Figure 5a) and the CX-1 line that expresses predominantly *NANOGP8*. The potential candidate should be the shRNA that inhibits *NANOGP8* in CX-1 and has less effect on *NANOG* in PA-1. shNp8-1 did not inhibit the expression of *NANOG* transcripts in PA-1 whereas the shNg-1 did (Figure 6a). In contrast, shNp8-1 inhibited the more prevalent *NANOGP8* transcripts in CX-1 (Figure 6b). When tested for their ability to inhibit single cell spherogenicity

in CRC, shNp8-1 significantly inhibited sphere formation in 3 cell lines (Figures 5c-e) whereas shNg-1 did not.

In addition, stem cells are frequently identified as the ‘‘side population’’ (SP) based on ABCG2-mediated efflux of Hoechst dye (31). We could not measure the SP fraction of MIP-101, Clone A and LS 174T because the inhibitor did not block dye efflux even at high concentrations without toxicity to the cells (data not shown), so we did SP analysis in CX-1 and KM-12c lines. The expression of ES TFs was first analyzed in CX-1, SP and Non-SP by qRT-PCR. Relative expression of the TF transcripts were consistently increased in SP 2 – 3-fold compared to Non-SP and parental CX-1 cells (Supplementary Figure 5b). In order to investigate whether *NANOGP8* can affect the size of the SP fraction, we transduced the CX-1 and KM- 12c CRC lines with shNp8-1 to inhibit *NANOGP8* or overexpressing *NANOG* or *NANOGP8* and measured the SP fraction. Allele-specific inhibition of *NANOGP8* reduced the size of the SP by more than 50% compared to the untreated parental line, while overexpression of *NANOGP8* increased the SP fraction by 2 – 4 fold in these two CRC lines (Figures 6f and g; Supplementary Figures 6 and 7).

We then tested whether inhibition of *NANOGP8* by shNP8-1 inhibited tumorigenicity in mice. Clone And CX-1 were transduced in vitro for 7 days and then injected into groups of 10 NOD/SCID mice at 10^5 cells per mouse mice that were sacrificed 26 (CX-1, Figures 6 h and i) or 31 (Clone A, Figure 6j) days later, tumors harvested and weighed. CX-1 and Clone A transduced with shNp8-1 were significantly lighter than the other groups (Figures 6i and j) with 30% of CX-1 and 40% of Clone A shNp8-1 treated mice tumor free (Figures h –j). Thus, inhibition of *NANOGP8* inhibits tumorigenicity in CRC in both CX-1 and Clone A.

Discussion

Our data support the role of *NANOG* in modulating stemness in human CRC as measured by single cell spherogenicity, the fraction of the side population and growth in vivo in immunoincompetent mice. Inhibition of *NANOG* expression within CRC generally decreased these effects while over-expression of *NANOG* or *NANOGP8* had the opposite outcome. These data indicated that *NANOG* expression can induce a stem-like state in CRC, which is consistent with the *NANOG* function reported in prostate cancer (14), OCT4 in melanoma cells (32) and *SOX2* in breast cancer cells (33). It is interesting that any one of these three ES TFs is enough to induce differentiated cancer cells to a stem-like state. One possible explanation is that NANOG, OCT4 and SOX2 individually and together can initiate and support the reprogramming process by activating their embryonic transcriptional factor networks (34-37).

Expression of OCT4 and SOX2 is associated with clinical outcome in various human malignancies including lung (38), esophageal (39, 40), ovarian (41), cervical (42) and gastric (43) carcinomas. Expression of *NANOG* has been identified as a component of an embryonic stem cell signature in various human carcinomas (16, 44-46). NANOG interacts with the Hedgehog pathway (16) and epithelial-mesenchymal transition (18, 47, 48) where *NANOG* may play a role in maintaining pluripotency that is necessary for generating tumor heterogeneity. Thus, *NANOG* expression may be a critical co-factor for neoplastic progression.

NANOG is expressed in primary colon carcinomas but expression was not associated with stage of disease or survival in one study (17). However, Meng *et al*. (18) reported an association between NANOG protein expression and clinical outcome in CRC. This difference may be because *NANOG* is expressed at low levels since a whole transcriptome analysis library contained fewer than 500 reads for NANOG-related transcripts in human CRC lines that generated 10 – 40 million reads (data not shown). Alternatively, *NANOG*-related mRNAs may also have a regulatory function as suggested by Salmena *et al*. (49). Interestingly, Ishiguro *et al.* (19) confirmed that NANOG protein levels in primary colorectal carcinomas were associated with both stage of disease and overall survival.

Our data also confirm and extend those of others (12-16, 20) that the *NANOG* involved in malignancy is often not the prototypic embryonic gene located on chromosome 12 identified

by Chambers *et al*. (50) but rather *NANOGP8*, a retrogene located on chromosome 15 identified by Booth and Holland (23). We found that NANOG and NanogP8 are often co-expressed but it is not clear how *NANOGP8* expression is regulated, only that *NANOGP8* expression may rescue stemness characteristics when *NANOG* is inhibited. Moreover, inhibition of *NANOG* gene expression is associated with inhibition of cell proliferation. Since Wee1 is an important regulator of the cell cycle and also inhibition of *NANOG* decreased Wee1, this may be an important aspect of how inhibition of *NANOG* may inhibit the malignant phenotype. We also found both NANOG and Pin 1 are located in the perinuclear space in the cytoplasm where they may interact to affect cell proliferation and maintain the stemness of CRC.

In summary, the present study extends previous work in that we show NANOGP8 is translated and may substitute for NANOG to maintain the stem cell characteristics of the human CRC as measured by the in vitro correlates of spherogenicity and the size of the side population. It is not clear why the response of CX-1 cells to overexpression of NANOG is not able to 'rescue' spherogenicity or why the relative levels of *NANOG* transcripts are not as prevalent as in the Clone A line. However, Jeter et al. (14) observed similar variations in response to overexpression of *NANOG*. Further work is necessary to elucidate the difference in response and control of expression of the *NANOG*s.

Materials and methods

Reagents

Unless specified, all reagents were obtained from Sigma (Sigma-Aldrich, St. Louis, MO, USA).

RT-PCR, Restriction Endonuclease Digestion and qRT-PCR

Total RNA from CRC cell lines (Clone A, CX-1, KM-12c, MIP-101, LS-174T and HCC-2998) was extracted using RNeasy Mini Kit (Qiagen, Valencia, CA, USA). Total RNA from CRC clinical samples was extracted using RecoverAll Total Nucleic Acid Isolation Kit (Ambion, Austin, TX, USA). Total RNA was treated with RNase-free DNase Set (Qiagen). The reverse transcription (RT) reaction was carried out with 2 µg total RNA in a 20 µl reaction using SuperScript III first strand synthesis system (Invitrogen, Carlsbad, CA, USA). 20 µl PCR products digested with AlwNI according to the manufacturer's protocol (New England Biolabs, Beverly, MA, USA) were analyzed by electrophoresis on a 3% (w/v) agarose gel. PCR products were sequenced after TA cloning. Real-time quantitative PCR (qRT-PCR) analysis was performed with IQ5 (Bio-rad, Hercules, CA, USA) thermal cycler in a 96 well plate. Expression level of human GAPDH was used as internal control. Relative gene expression levels were calculated with $2^{-\Delta\Delta CT}$ method.

Cell Culture, Cell Transfection, Lentivirus Packaging and Cell Transduction

The human CRC cells were cultured in RPMI (Invitrogen) media supplemented with 10% FBS (Invitrogen) and 2mM L-glutamine (Invitrogen) at 37°C, 5% CO_2 incubator. Stable transductants were created by puromycin selection for shNANOG and pLKO.1 with lentiviral particles from Sigma (shNANOG was TRCN0000004885). The other shRNA lentiviral vectors used the Clone-it enzyme-free lentivector system (System Biosciences, Mountain View, CA, USA) containing the COP-GFP reporter with DNA oligonucleotides from Integrated DNA Technologies (Coralville, IA). Zhang et. (12 2006) provided the fulllength NANOG plasmid DNA and full length NANOGP8 was amplified from Clone A and confirmed by sequencing. Lentiviral particles to express full length NANOG or NANOGP8 were ligated with the Clone-it enzyme free lentivectors with a RFP reporter (System Biosciences). The allele specific shRNAs were shNg-1 to *NANOG* (target sequence 5'-CUGCAUGCAGUUCCAGCCA-3'), shNp8-1 to *NANOGP8* (target sequence 5'-

CUGCAUGCACUUCCAGCCA-3') with the control vector shNeg (target sequence 5'-UAGCGACUAAACACAUCAA-3' (51). Lentiviral particles were produced by co-transfection of 293T cells with packaging and envelope plasmids using Lipofectamine 2000 (Invitrogen).

Sphere Culture

Cells were plated in ULLA plates (Corning Incorporated, Corning, NY, USA) using serum-free medium (52). For single cell spherogenicity assay, cells were cultured in 96-well ULLA plates at a rate of 0.6 cell/well in serum-free medium and wells containing single cells identified within 24 hours. Spheroids containing more than 50 cells were scored after 9 or more days.

Cell Proliferation Analysis

$2x10^3$ (per well) CRC cells were grown in 96-well plates for 48 hours and 10 µl/well cell proliferation reagent WST1 (Roche Applied Sciences, Indianapolis, IN, USA) was added and then measure the absorbance at 450nm after 4 hours.

Side Population Analysis

Side population was analyzed according to the method of Lin and Goodell (53). Side population was performed on BDLSRII flow cytometer (Becton Dickinson, San Jose, CA, USA) using BD FACSDiva software.

Immunoprecipitation, Mass Spectrometry Analysis and Western blot

Immunoprecipitation was performed using Protein G Sepharose 4 Fast Flow (GE Healthcare, Pittsburgh, PA, USA). For mass spectrometry assay, the gel band was excised from the region on SDS-PAGE corresponding to NANOG molecular weight and to the NANOG signal on western blot. Mass spectrometry analysis was performed as described (54). For Western blot analysis, protein (50 µg) was separated in Nu-PAGE 4-12% Bis-Tris Gel (Invitrogen) and transferred onto a polyvinylidene difluoride (PVDF) in Tris-Glycine Transfer Buffer (Invitrogen). The membrane was blocked with 5% milk and then incubated with antibodies against anti- phosphor-Wee1 (4910, Cell Signaling), anti-Wee1 (4936, Cell Signaling), anti-phosphor-Cdc2 (AF888, R&D

Systems, Minneapolis, MN, USA), anti-Cdc2 (9112, Cell Signaling), anti-phosphor-Chk1 (ab47318, Abcam, Cambridge, MA, USA), anti-Chk1 (ab47574, Abcam), anti-phosphor-Cdc25C (ab32051, Abcam), anti-Cdc25C (ab2359, Abcam), anti-Pin1 (3722, Cell Signaling), anti-Nanog (AF1997, R & D Systems and 4893 and 4903, Cell Signalling) and anti- β-Tubulin (T4026, Sigma-Aldrich) and subsequently washed and incubated with a specific secondary antibody (NA931V and NA934V, GE Healthcare). Protein loading was normalized against β-Tubulin.

Immunofluorescence Assay

De-identified formalin-fixed paraffin embedded specimens of liver metastases from colon carcinoma were obtained from the Pathology Service of the Center for Cancer Research under exemption #5426 from the NIH Office of Human Subjects. Sections 5 μ thick were microdissected and RNA extracted for RT-PCR and analyzed for the presence of NANOGP8 transcripts as described above. In addition, companion 5 μ sections were analyzed for the expression of NANOG (AF1997, R &D Systems) and CD44v6 (BBA13, R&D Systems) by immunofluorescence assay at 1:100 dilutions with DAPI nuclear counter stains. Positive controls included similar sections of formalin-fixed paraffin-embedded human seminoma. Staining was performed as described (55).

In Vivo Tumorigenic, Metastatic Potential Assays

Animal experiments were preformed under the protocol LEC-011 approved by the NCI Animal Care and Use Committee. Parental cells, cells with pLKO.1 and cells with shRNA to *NANOG* or *NANOGP8* (shNANOG, shNg-1, shNp8-1) were injected subcutaneously into NOD/SCID mice. The potential of cell lines to form experimental metastases in the liver was examined in NOD/SCID mice by inoculation of tumor cells into the spleen during open laparotomy under flurane anesthesia. Autopsies were performed and the presence of liver metastases was determined by macroscopic inspection and confirmed by histological analysis.

Statistical Analysis

ANOVA or contingency table analysis with Bonferroni correction was performed for statistical analysis of multiple comparisons. Data in graphs are presented as mean ± S.D. except where indicated in the text. For the analyses, $P<0.05$ was considered to be statistically significant.

Conflict of interest

The authors declare no conflict of interest.

Acknowledgements

The authors acknowledge the valuable advice and support of Drs. Elizabeth Conner and Valentina Factor. Also the authors gratefully acknowledge the support provided by the Center for Cancer Research of the NCI for Project ZIA BC 011199 and by the Department of Defense for Grant Number W81XWH-11-1-0327. The opinions expressed in this manuscript are those of the authors and do not necessarily represent those of the National Cancer Institute, the National Institutes of Health, the Department of Health and Human Services or the Department of the Army.

Supplementary Information accompanies the paper on the Oncogene website (http://www.nature.com/onc)

References

1. Takahashi K, Yamanaka S. Induction of pluripotent stem cells from mouse embryonic and adult fibroblast cultures by defined factors. *Cell* 2006; **126:** 663-676.

2. Takahashi K, Tanabe K, Ohnuki M, Narita M, Ichisaka T, Tomoda K *et al*. Induction of pluripotent stem cells from adult human fibroblasts by defined factors. *Cell* 2007; **131**: 861-872.

3. Yu J, Hu K, Smuga-Otto K, Tian S, Stewart R, Slukvin II *et al*. Human induced pluripotent stem cells free of vector and transgene sequences. *Science* 2009; **324**: 797-801.

4. Park IH, Arora N, Huo H, Maherali N, Ahfeldt T, Shimamura A *et al*. Disease-specific induced pluripotent stem cells. *Cell* 2008; **134**: 877-886.

5. Miyoshi N, Ishii H, Nagai K, Hoshino H, Mimori K, Tanaka F *et al*. Defined factors induce reprogramming of gastrointestinal cancer cells. *Proc Natl Acad Sci U S A* 2010; **107**: 40-45.

6. Silva J, Nichols J, Theunissen TW, Guo G, van Oosten AL, Barrandon O *et al*. NANOG is the gateway to the pluripotent ground state. *Cell* 2009; **138**: 722-737.

7. Mitsui K, Tokuzawa Y, Itoh H, Segawa K, Murakami M, Takahashi K *et al*. The homeoprotein NANOG is required for maintenance of pluripotency in mouse epiblast and ES cells. *Cell* 2003; **113**: 631-642.

8. Chambers I, Silva J, Colby D, Nichols J, Nijmeijer B, Robertson M *et al*. NANOG safeguards pluripotency and mediates germline development. *Nature* 2007; **450**: 1230-1234.

9. Lengner CJ, Camargo FD, Hochedlinger K, Welstead GG, Zaidi S, Gokhale S *et al*. Oct4 expression is not required for mouse somatic stem cell self-renewal. *Cell Stem Cell* 2007; **1**: 403-415.

10. Utikal J, Maherali N, Kulalert W, Hochedlinger K. Sox2 is dispensable for the reprogramming of melanocytes and melanoma cells into induced pluripotent stem cells. *J Cell Sci* 2009; **122**: 3502-3510.

11. Miyanari Y, Torres-Padilla ME. (2012). Control of ground-state pluripotency by allelic regulation of NANOG. *Nature* **483**: 470-473.

12. Zhang J, Wang X, Li M, Han J, Chen B, Wang B *et al*. NANOGP8 is a retrogene expressed in cancers. *FEBS J* 2006; **273**: 1723-1730.

13. Jeter CR, Badeaux M, Choy G, Chandra D, Patrawala L, Liu C *et al*. Functional evidence that the self-renewal gene NANOG regulates human tumor development. *Stem Cells* 2009; **27**: 993-1005.

14. Jeter CR, Liu B, Liu X, Chen X, Liu C, Calhoun-Davis T *et al*. NANOG promotes cancer stem cell characteristics and prostate cancer resistance to androgen deprivation. *Oncogene* 2011; **30**: 3833-3845.

15. Po A, Ferretti E, Miele E, Smaele ED, Paganelli A, Canettieri G *et al*. Hedgehog controls neural stem cells through p53-independent regulation of NANOG. *EMBO J* 2010; **29**: 2646-2658.

16. Zbinden M, Duquet A, Lorente-Trigos A, Ngwabyt SN, Borges I, Ruiz i Altaba A. NANOG regulates glioma stem cells and is essential in vivo acting in a cross-functional network with GLI1 and p53. *EMBO J* 2010; **29**: 2659-2674.

17. Saiki Y, Ishimaru S, Mimori K, Takatsuno Y, Nagahara M, Ishii H *et al*. Comprehensive analysis of the clinical significance of inducing pluripotent stemness-related gene expression in colorectal cancer cells. *Ann Surg Oncol* 2009; **16**: 2638-2644.

18. Meng HM, Zheng P, Wang XY, Liu C, Sui HM, Wu SJ *et al*. Overexpression of NANOG predicts tumor progression and poor prognosis in colorectal cancer. *Cancer Biol Ther* 2010; **9**: 295-302.

19. Ishiguro T, Sato A, Ohata H, Sakai H, Nakagama H, Okamoto K. Differential expression of NANOG1 and NANOGp8 in colon cancer cells. *Biochem Biophys Res Commun.* 2012; **418**:199-204.

20. Xu F, Dai C, Zhang R, Zhao Y, Peng S, Jia C. NANOG: A Potential Biomarker for Liver Metastasis of Colorectal Cancer. Dig Dis Sci. 2012 May 6. [Epub ahead of print] DOI: 10.1007/s10620-012-2182-8.

21. Eberle I, Pless B, Braun M, Dingermann T, Marschalek R. Transcriptional properties of human NANOG1 and NANOG2 in acute leukemic cells. *Nucleic Acids Res* 2010*;* **38:** 5384-5395.

22. Mulder JW, Kruyt PM, Sewnath M, Oosting J, Seldenrijk CA, Weidema WF *et al*.

Colorectal cancer prognosis and expression of exon-v6-containing CD44 proteins. *Lancet* 1994; **344**: 1470-1472.

23. Booth HA, Holland PW. Eleven daughters of NANOG. *Genomics* 2004; **84**: 229-238.

24. Ambady S, Malcuit C, Kashpur O, Kole D, Holmes WF, Hedblom E *et al*. Expression of NANOG and NANOGP8 in a variety of undifferentiated and differentiated human cells. *Int J Dev Biol* 2010; **54**: 1743-1754.

25. Zhang J, Jessup JM, Thorgeirsson SS. NANOG family members are essential for spherogenicity and metastasis in colorectal carcinoma. In: Proceedings of the 102nd Annual Meeting of the American Association for Cancer Research; 2011 Apr 2-6; Orlando, Florida. Philadelphia (PA): AACR; 2011. Abstract 5206.

26. Jessup JM, Giavazzi R, Campbell D, Cleary KR, Morikawa K, Hostetter R *et al*. Metastatic potential of human colorectal carcinomas implanted into nude mice: prediction of clinical outcome in patients operated upon for cure. *Cancer Res* 1989; **49**: 6906-6910.

27. Lu KP, Hanes S D, Hunter T. A human peptidyl-prolyl isomerase essential for regulation of mitosis. *Nature* 1996; **380**, 544−547.

28. Nishi M, Akutsu H, Masui S, Kondo A, Nagashima Y, Kimura H *et al*. A distinct role for Pin1 in the induction and maintenance of pluripotency. *J Biol Chem* 2011; **286**: 11593-11603.

29. Huang H, Qiao R, Zhao D, Zhang T, Li Y, Yi F *et al*. Profiling of mismatch discrimination in RNAi enabled rational design of allele-specific siRNAs. *Nucleic Acids Res* 2009; **37**: 7560-7569.

30. Dykxhoorn DM, Schlehuber LD, London IM, Lieberman J. Determinants of specific RNA interference-mediated silencing of human beta-globin alleles differing by a single nucleotide polymorphism. *Proc Natl Acad Sci U S A* 2006; **103**: 5953-5958.

31. Goodell MA, Brose K, Paradis G, Conner AS, Mulligan RC. Isolation and functional properties of murine hematopoietic stem cells that are replicating in vivo. *J Exp Med* 1996; **183**: 1797-1806.

32. Kumar SM, Liu S, Lu H, Zhang H, Zhang PJ, Gimotty PA *et al*. (2012). Acquired cancer stem cell phenotypes through Oct4-mediated dedifferentiation. *Oncogene*, advance online publication 30 January 2012; doi: 10.1038/onc.2011.656.

33. Leis O, Eguiara A, Lopez-Arribillaga E, Alberdi MJ, Hernandez-Garcia S, Elorriaga K *et al*. Sox2 expression in breast tumours and activation in breast cancer stem cells. *Oncogene* 2012; **31**: 1354-1365.

34. Boyer LA, Lee TI, Cole MF, Johnstone SE, Levine SS, Zucker JP *et al*. Core transcriptional regulatory circuitry in human embryonic stem cells. *Cell* 2005; **122**: 947-956.

35. Chen X, Xu H, Yuan P, Fang F, Huss M, Vega VB *et al*. Integration of external signaling pathways with the core transcriptional network in embryonic stem cells. *Cell* 2008; **133**: 1106-1117.

36. Kim J, Chu J, Shen X, Wang J, Orkin SH. An extended transcriptional network for pluripotency of embryonic stem cells. *Cell* 2008; **132**: 1049-1061.

37. Ding J, Xu H, Faiola F, Ma'ayan A, Wang J. Oct4 links multiple epigenetic pathways to the pluripotency network. *Cell Res* 2012; **22**: 155-167.

38. Sholl LM, Barletta JA, Yeap BY, Chirieac LR, Hornick JL. Sox2 protein expression is an independent poor prognostic indicator in stage I lung adenocarcinoma. *Am J Surg Pathol* 2010; **34**: 1193-1198.

39. Bass AJ, Watanabe H, Mermel CH, Yu S, Perner S, Verhaak RG *et al*. SOX2 is an amplified lineage-survival oncogene in lung and esophageal squamous cell carcinomas. *Nat Genet* 2009; **41**: 1238-1242.

40. Wang Q, He W, Lu C, Wang Z, Wang J, Giercksky KE *et al*. Oct3/4 and Sox2 are significantly associated with an unfavorable clinical outcome in human esophageal squamous cell carcinoma. *Anticancer Res* 2009; **29**: 1233-1241.

41. Zhang J, Li YL, Zhou CY, Hu YT, Chen HZ. Expression of octamer-4 in serous and mucinous ovarian carcinoma. J Clin Pathol 2010; **63**: 879-883.

42. Ji J, Zheng PS. Expression of Sox2 in human cervical carcinogenesis. *Hum Pathol* 2010; **41**: 1438-1447.

43. Zhang X, Yu H, Yang Y, Zhu R, Bai J, Peng Z *et al*. SOX2 in gastric carcinoma, but not Hath1, is related to patients' clinicopathological features and prognosis. *J Gastrointest Surg* 2010; **14**: 1220-1226.

44. You JS, Kang JK, Seo DW, Park JH, Park JW, Lee JC *et al*. Depletion of embryonic stem cell signature by histone deacetylase inhibitor in NCCIT cells: involvement of NANOG suppression. *Cancer Res* 2009; **69**: 5716-5725.

45. Ben-Porath I, Thomson MW, Carey VJ, Ge R, Bell GW, Regev A *et al*. An embryonic stem cell-like gene expression signature in poorly differentiated aggressive human tumors. *Nat Genet* 2008; **40**: 499-507.

46. Santagata S, Ligon KL, Hornick JL. Embryonic stem cell transcription factor signatures in the diagnosis of primary and metastatic germ cell tumors. *Am J Surg Pathol* 2007; **31:** 836-845.

47. Katoh M. Network of WNT and other regulatory signaling cascades in pluripotent stem cells and cancer stem cells. *Curr Pharm Biotechnol* 2011; **12**: 160-170.

48. Kong D, Banerjee S, Ahmad A, Li Y, Wang Z, Sethi S *et al*. Epithelial to mesenchymal transition is mechanistically linked with stem cell signatures in prostate cancer cells. *PLoS One* 2010; **5**: e12445.

49. Salmena L, Poliseno L, Tay Y, Kats L, Pandolfi PP. A ceRNA hypothesis: the Rosetta Stone of a hidden RNA language? *Cell* 2011; **146**: 353-358.

50. Chambers I, Colby D, Robertson M, Nichols J, Lee S, Tweedie S *et al*. Functional expression cloning of NANOG, a pluripotency sustaining factor in embryonic stem cells. *Cell* 2003; **113**: 643-655.

51. Huang H, Regan KM, Lou Z, Chen J, Tindall DJ. CDK2-dependent phosphorylation of FOXO1 as an apoptotic response to DNA damage. *Science* 2006 13; **314**:294-7

52. Zappone MV, Galli R, Catena R, Meani N, De Biasi S, Mattei E *et al*. Sox2 regulatory sequences direct expression of a (beta)-geo transgene to telencephalic neural stem cells and precursors of the mouse embryo, revealing regionalization of gene expression in CNS stem cells. *Development* 2000; **127:** 2367-2382.

53. Lin KK, Goodell MA. Purification of hematopoietic stem cells using the side population. *Methods Enzymol* 2006; **420**: 255-264.

54. Simkus C, Bhattacharyya A, Zhou M, Veenstra TD, Jones JM. Correlation between recombinase activating gene 1 ubiquitin ligase activity and V(D)J recombination. *Immunology* 2009; **128**, 206-217.

55. Kinders RJ, Hollingshead M, Lawrence S, Ji J, Tabb B, Bonner WM *et al*. Development of a validated immunofluorescence assay for γH2AX as a pharmacodynamic marker of topoisomerase I inhibitor activity. *Clin Cancer Res* 2010; **16**: 5447-5457.

Figure Legends

Figure 1 The Retrogene NANOGP8 is Upregulated in Clinical Samples

(a-b) 5 μ formalin-fixed paraffin embedded specimens of liver metastases sections were analyzed for the expression of NANOG protein and CD44v6 by immunofluorescence assay (IFA) that included DAPI nuclear counter stains. Patient 9 (whose tumor expressed only *NANOGP8* transcripts) (a) is shown. Positive controls included similar sections of formalin-fixed paraffin-embedded human seminoma that is known to express nuclear NANOG (b). Images were captured on a Nikon 90i microscope with a DU888 EMCCD camera and analyzed with NIS-Elements software. Object magnification, 20X. White Bars are 10 microns.

(c) The restriction endonuclease that distinguishes the two genes is AlwNI, an enzyme that identifies a palindromic hexanucleotide sequence in *NANOGP8* but not *NANOG* at position 144 relative to the translational start site.

(d-f) Sections from liver metastases that had been resected were microdissected and total RNA prepared from tumor and adjacent normal liver. RT-PCR products were run out on agarose gels and GAPDH as an internal control and 8 metastatic tumors (T) and 4 adjacent microscopically normal liver samples (N) contained *NANOG* transcripts (d). When the positive cDNAs from Panel d were subjected to digestion with AlwNI, 6 tumor samples and 1 adjacent liver contained *NANOGP8* (e-f). These results were confirmed by direct sequencing (data not shown). The relative *NANOGP8* expression is calculated as the ratio between densitometry reading of *NANOGP8* and total *NANOG* by using Image J software. Abbreviations: M, 100bp DNA ladder marker; bp, base pair; UD, undigested; D, digested with AlwNI; N, adjacent normal liver sample; T, tumor sample; +, positive; -, negative.

Figure 2 *NANOGP8* is Prevalent Form of *NANOG* Expressed in CRC Lines

(a-b) Total RNA was extracted and qRT-PCR was performed for embryonic stem cell TFs. The results were normalized to GAPDH and HCC 2998 monolayers. Mean % ± SD.

(c-d) Restriction endonuclease digestion of 260 nt length of *NANOG* by RT-PCR amplifies a region where there is a SNP that identifies *NANOGP8*. Digestion with AlwNI reveals that even in

monolayer culture *NANOGP8* is frequently expressed in CRC lines (c) as well as in spheroids (d). The relative *NANOGP8* expression is calculated as the ratio between densitometry reading of *NANOGP8* and total *NANOG* by using Image J software. Direct sequencing confirmed that *NANOGP8* is consistently upregulated in Clone A and CX-1 spheroids (e). Numbers in (e) stand for the numbers of *NANOG* or *NANOGP8* in sequenced clones.

(f) MS/MS spectrum of a NANOGP8 tryptic peptide GKQPTSAENSVAK. This peptide is unique to NANOGP8, which includes the shift from Lys (K) in NANOG to Asn (N) in NANOGP8 at codon 82.

Abbreviations: M, 100bp DNA ladder marker; bp, base pair; UD, undigested; D, digested with AlwNI.

Figure 3 Modulation of NANOG Gene Expression Affects Spherogenicity in CRC Lines

(a) Single cells were cultured in serum-free medium in ULLA microtiter plates for 9 days and then scored for the number of spheroids that each single cell produced (Mean ± SD of % of single cells that formed spheroids of 50 or more cells). All CRC lines formed spheroids at frequencies that ranged from 1 – 56% of single cells plated.

(b) Western blot of NANOG in parental cells, control vector (pLKO.1) and shNANOG transduced Clone A, CX-1.

(c-d) Single cells forming spheroids were scored in Clone A (c) and CX-1 (d) transduced with lentiviral vectors containing shRNA to NANOG, pLKO.1, full length NANOG, or full length NANOGP8. shNANOG inhibited spheroid formation in both CRC compared to the parental cells. In addition, shNanog cells were secondarily transduced with Nanog or NANOGP8 for 5 days before culture for single cell spherogenicity or evaluation of transcript expression. Recovery of *NANOGP8* either in Clone A or CX-1 transduced shNANOG restored the single cell spherogenicity. Mean ± SD of single cells forming spheroids of 50 or more cells.

(e-f) Restriction endonuclease digestion of 260 nt length of *NANOG* by RT-PCR amplifies a region where there is a single nucleotide alteration that identifies NANOGP8. Digestion with AlwNI reveals that shNANOG inhibits NANOG and transduction with either lentiviral vector *NANOG* or *NANOGP8* increased *NANOG* or *NANOGP8* trancripts, respectively. The relative *NANOGP8* expression is calculated as the ratio between densitometry reading of *NANOGP8* and

total *NANOG* by using Image J software. Abbreviations: M, 100bp DNA ladder marker; bp, base pair; UD, undigested; D, digested with AlwNI.

Figure 4 shNANOG Inhibits Tumorigenicity and Experimental Metastasis

(a-b) Groups of 5 – 10 NOD/SCID mice were injected with dilutions of 10^3–10^5 viable CX-1 cells subcutaneously in NOD/SCID mice. Parental, pLKO.1 and shNANOG transductants were scored for the appearance of tumors over 70 days after tumor inoculation. shNANOG decreased tumorigenicity at each dilution (a). 10^5 CX-1 cells transducted with lentiviral vectors containing shRNA to NANOG, pLKO.1, or the intact NANOG coding sequence were injected into NOD/SCID mice. shNANOG decreases growth by prolonging the median days to appearance of tumors as well as the percentage of mice that are tumor free in mice injected with CX-1 cells (b). Overexpression of NANOG shortened the median number of days to tumor appearance compared to the pLKO.1 group (b).

(c) When 2 x 10^6 CX-1 cells were injected into the spleens of NOD/SCID mice, no shNANOG transduced CX-1 cells formed either gross or microscopic liver experimental metastases whereas 45 – 70% of mice injected with parental or control vector did. Error bars: SD . Experimental metastasis from Parental CX-1 did not generate fibrosis or host inflammatory response (data not shown).

Figure 5 shNANOG Induces Cell Cycle Inhibition in CRC

Clone A and CX-1 cells transduced with LV shNANOG, RFP control (RFP), full length NANOG or NANOGP8 were analyzed for cell proliferation (a, b) and expression of cell cycle-related proteins by Western blot (c). Controls were either the untreated parental CRC cell line or the pLKO.1 empty vector control. Wee1 protein expression is decreased in Clone A and CX-1 with a reduction in phosphorylation of cdc2, chk1, and CDC25C (c). P values by contingency table analysis with Bonferroni correction. * $P<0.05$ vs Parental Clone A or CX-1.

(d) Detection of the NANOG and Pin 1 in Clone A cells by IFA. Object magnification: 40X.

(e) The interaction of NANOG protein and Pin 1 in Clone A and Clone A transduced with NANOGP8 shown by reciprocal co-immunoprecipitation analysis. + and - refer to IP with or without primary antibody as negative controls in immunoprecipitation. IP, immunoprecipitation; WB, Western blotting.

Figure 6. Inhibition of NANOGP8 Inhibits Spherogenicity, Tumorigenicity and the size of Side Population in CRC Cells

(a-b) PA-1 is a human embryonal stem cell line that only expresses *NANOG* whereas CX-1 expresses both *NANOG* and *NANOG P8*. shNP8-1 did not decrease NANOG levels in PA-1 although shNg-1 did (a) but decreased transcript levels in CX-1 cells (b). Data normalized by GAPDH levels and levels of transcripts in the parental untreated line. P values after Bonferroni correction of contingency table analysis. * $P<0.01$ vs Parental PA-1 or CX-1.

(c-d) Effect of shRNA on single cell spherogenicity of Clone A (c), CX-1 (d), and LS 174T (e). shNP8-1 inhibited spherogenicity in all 3 CRC lines whereas shNg-1 did not. Mean % ± SD. P values by contingency table analysis with Bonferroni correction. P values after Bonferroni correction of contingency table analysis. ** $P <0.001$ vs Parental Clone A or CX-1.

(f-g) Detection of SP in CX-1 (g) and KM-12c (h) transduced with control (shNeg), shNp8-1, RFP control (RFP), the intact *NANOG* coding sequence (NANOG) or the *NANOGP8* coding sequence (NANOGP8). Mean % ± SD. P values by contingency table analysis with Bonferroni correction. * $P<0.01$ vs Parental CX-1 or KM-12c.

(h-j) Groups of 10 mice were injected with 10^5 cells per mouse transduced with lentiviral shRNA for 7 days or untreated tumor cells and then sacrificed at day 26 (CX-1 (h-i)) or day 31 (Clone A (j)). Five tumors are shown from each CX-1 group (h) and tumor weights are shown in (i-j). The dotted line is a cut-off of 75 mg with both CX-1 and Clone A transduced tumors weighing less than 75 mg whereas the untreated CX-1 (i) or Clone A (j) were heavier. P value by contingency table analysis with Bonferroni correction.

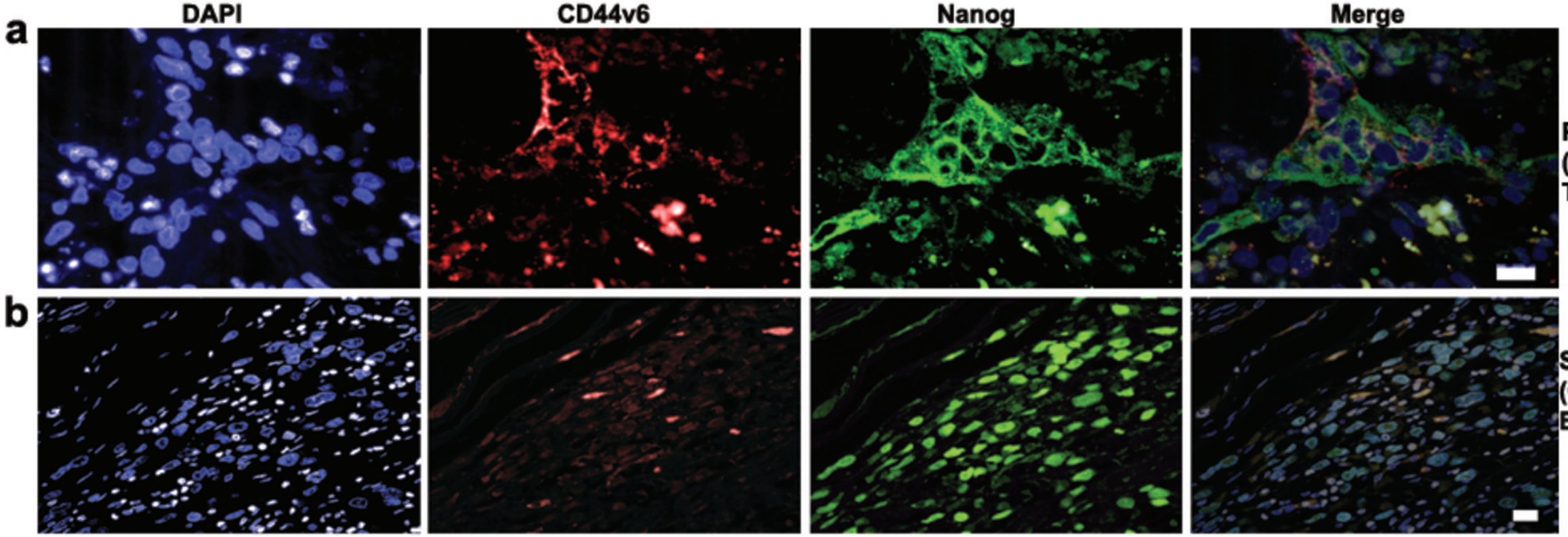

f

	Total Ng+	NP8 +	NP8 only	Ng only	Total Ng-	Total
Tumor	8	6	2	2	2	10
Adjacent Normal	4	1	0	3	6	10

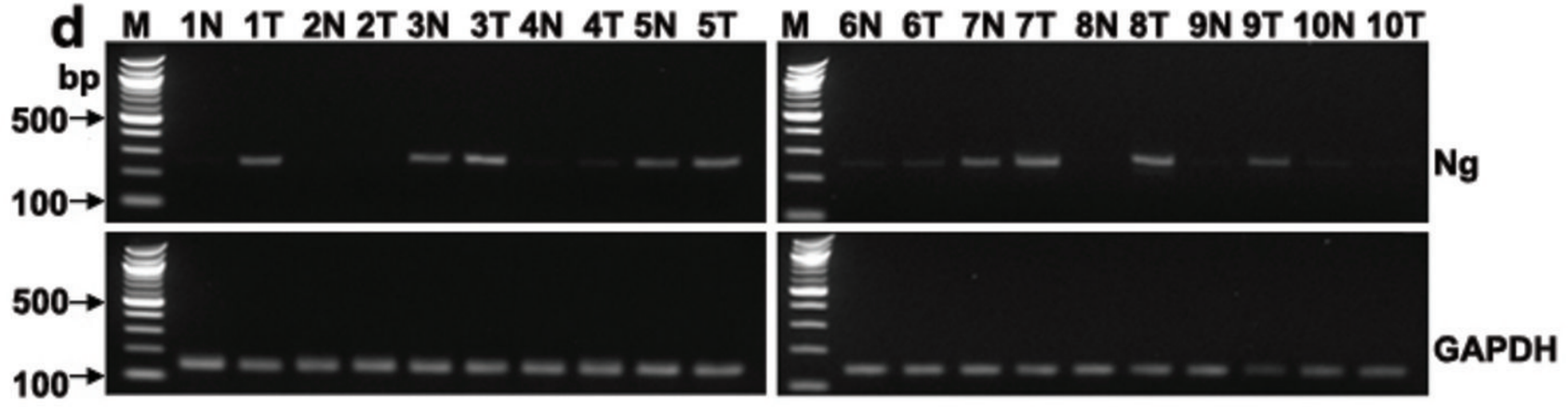

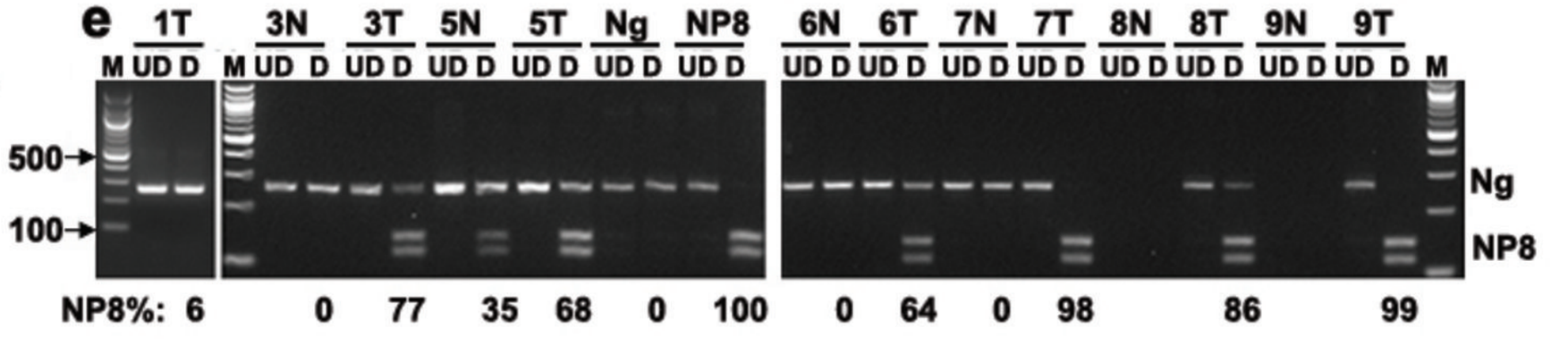

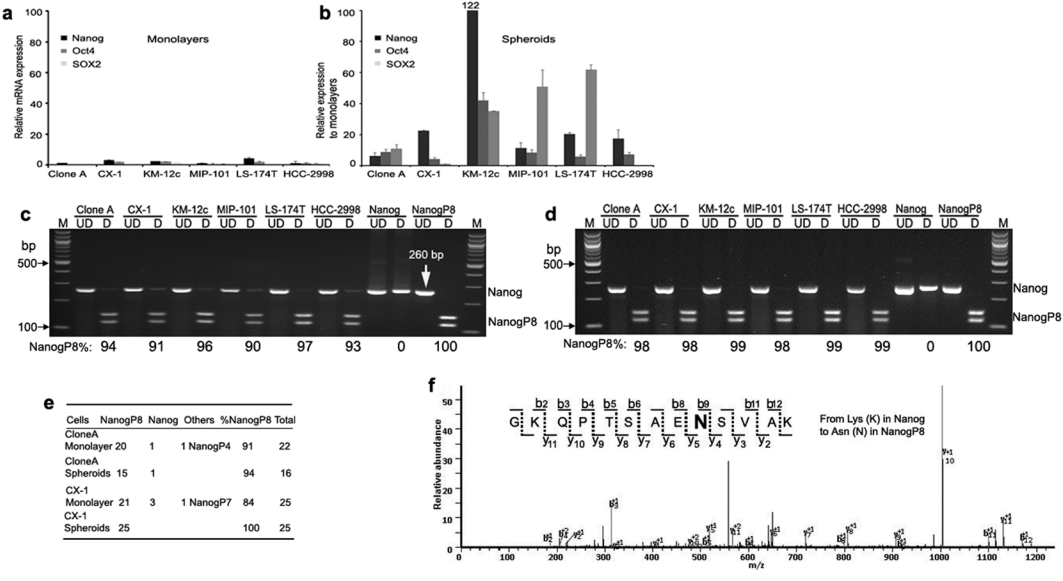
a
Relative mRNA expression
Nanog
Oct4
SOX2
Monolayers
Clone A
CX-1
KM-12c
MIP-101
LS-174T
HCC-2998
b
Relative expression to monolayers
122
Spheroids
c
M
UD
D
Nanog
NanogP8
bp
500
100
260 bp
NanogP8%: 94 91 96 90 97 93 0 100
d
NanogP8%: 98 98 99 98 99 99 0 100
e
Cells NanogP8 Nanog Others %NanogP8 Total
CloneA Monolayer 20 1 1 NanogP4 91 22
CloneA Spheroids 15 1 94 16
CX-1 Monolayer 21 3 1 NanogP7 84 25
CX-1 Spheroids 25 100 25
f
Relative abundance
m/z
From Lys (K) in Nanog to Asn (N) in NanogP8

Figure 2

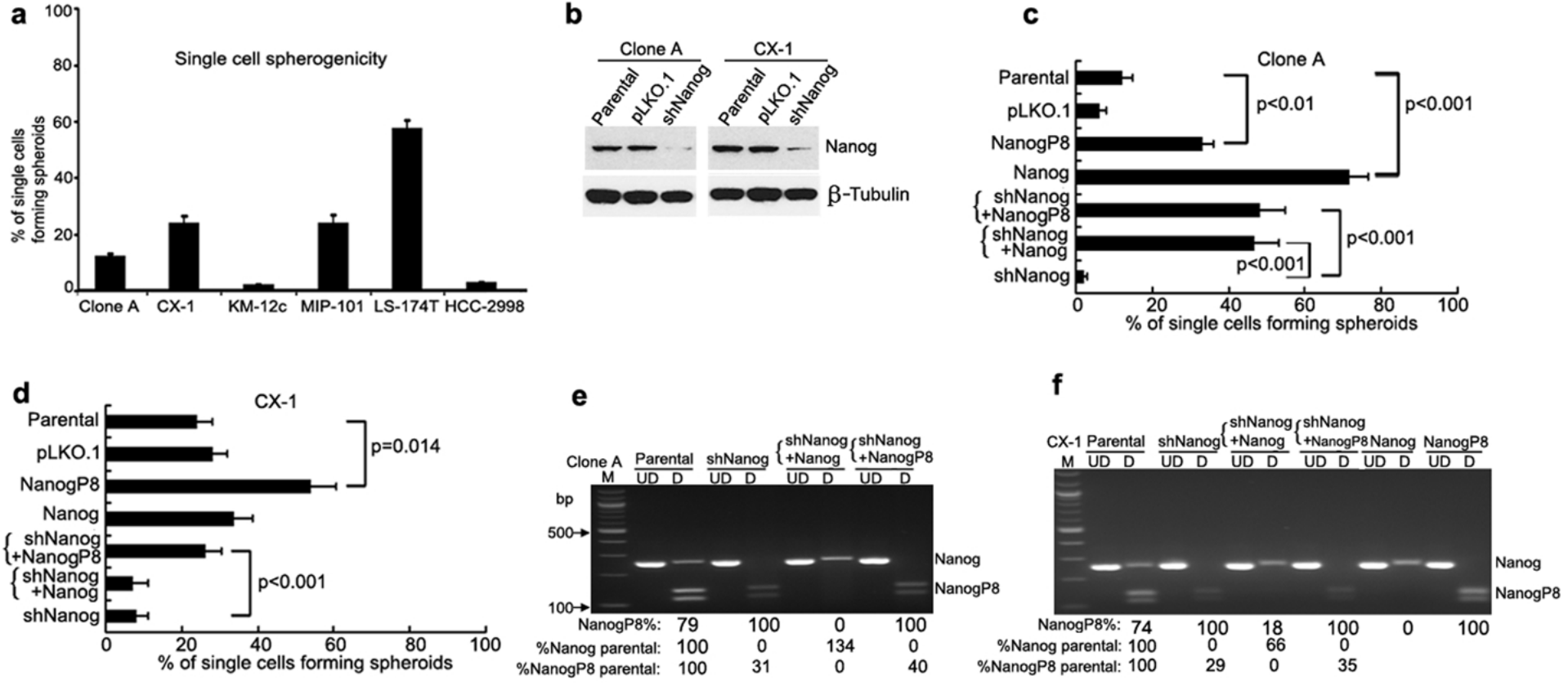
a
Single cell spherogenicity
% of single cells forming spheroids
Clone A
CX-1
KM-12c
MIP-101
LS-174T
HCC-2998
b
Clone A
CX-1
Parental
pLKO.1
shNanog
Nanog
β-Tubulin
c
Clone A
Parental
pLKO.1
NanogP8
Nanog
shNanog +NanogP8
shNanog +Nanog
shNanog
p<0.01
p<0.001
p<0.001
p<0.001
% of single cells forming spheroids
d
CX-1
Parental
pLKO.1
NanogP8
Nanog
shNanog +NanogP8
shNanog +Nanog
shNanog
p=0.014
p<0.001
% of single cells forming spheroids
e
Clone A
M
Parental
shNanog
shNanog +Nanog
shNanog +NanogP8
UD D
bp
500
100
Nanog
NanogP8
NanogP8%: 79 100 0 100
%Nanog parental: 100 0 134 0
%NanogP8 parental: 100 31 0 40
f
CX-1
M
Parental
shNanog
shNanog +Nanog
shNanog +NanogP8
Nanog
NanogP8
UD D
Nanog
NanogP8
NanogP8%: 74 100 18 100 0 100
%Nanog parental: 100 0 66 0
%NanogP8 parental: 100 29 0 35

Figure 3

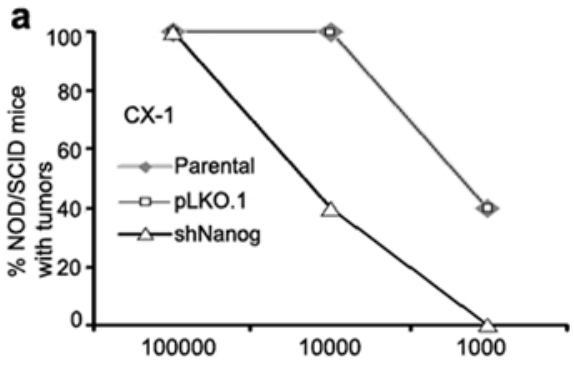

b

	Median (days)	p value	%Tumor free
Parental	30		0
pLKO.1	33	NS	0
shNanog	>50	<0.001	50
Nanog	18	<0.05	0
NanogP8	13	<0.005	0

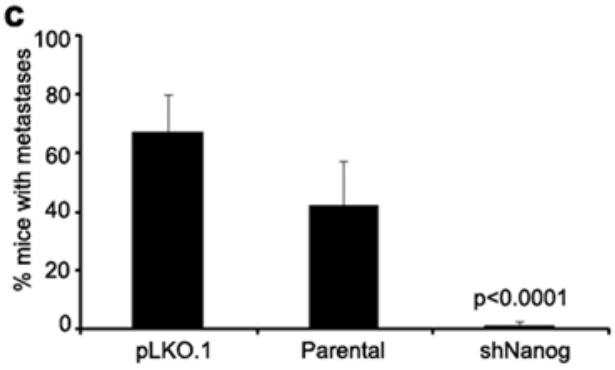

Figure 4

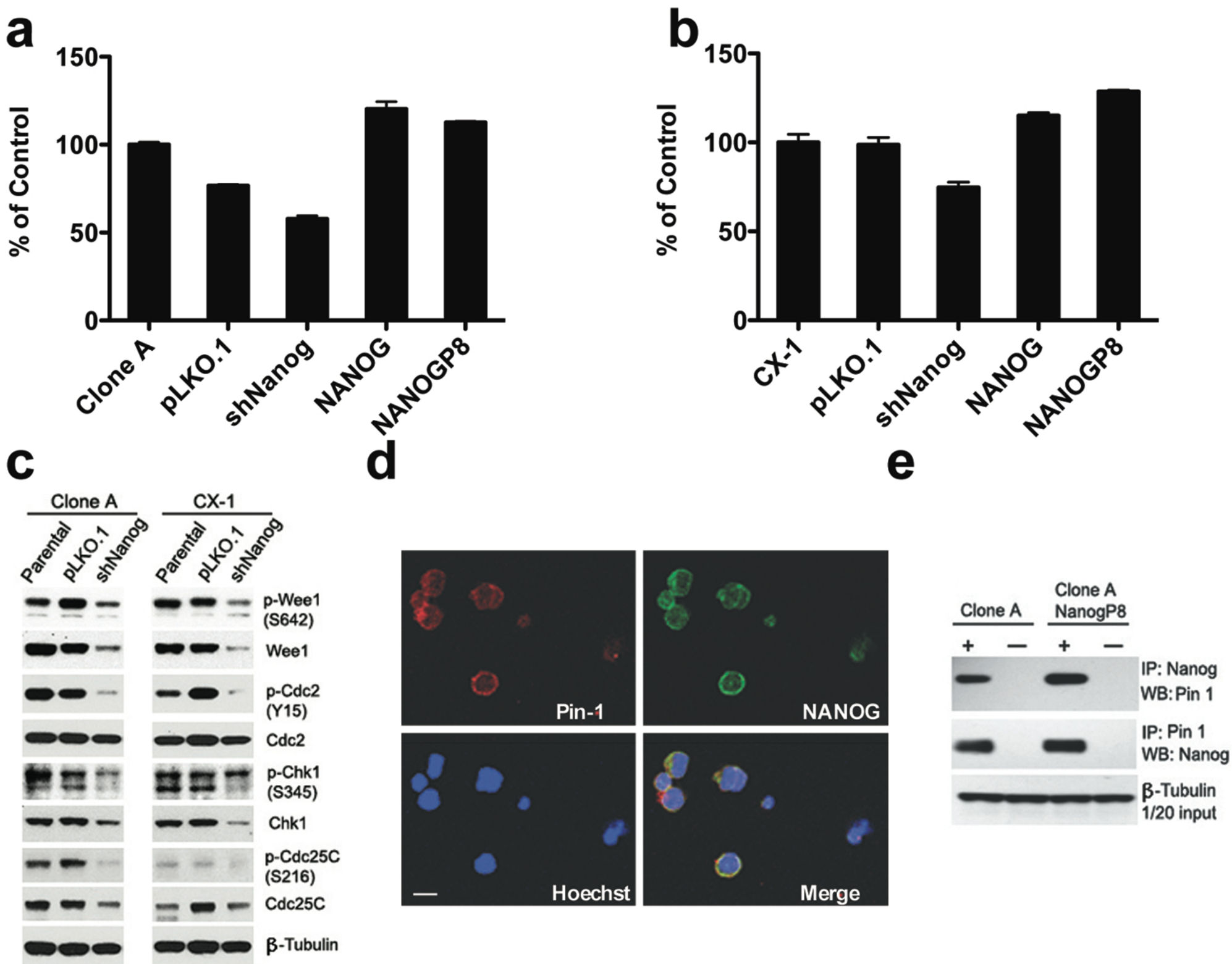
a
% of Control
150
100
50
0
Clone A
pLKO.1
shNanog
NANOG
NANOGP8
b
% of Control
150
100
50
0
CX-1
pLKO.1
shNanog
NANOG
NANOGP8
c
Clone A
CX-1
Parental
pLKO.1
shNanog
Parental
pLKO.1
shNanog
p-Wee1 (S642)
Wee1
p-Cdc2 (Y15)
Cdc2
p-Chk1 (S345)
Chk1
p-Cdc25C (S216)
Cdc25C
β-Tubulin
d
Pin-1
NANOG
Hoechst
Merge
e
Clone A
Clone A NanogP8
+
—
+
—
IP: Nanog
WB: Pin 1
IP: Pin 1
WB: Nanog
β-Tubulin
1/20 input

Figure 5

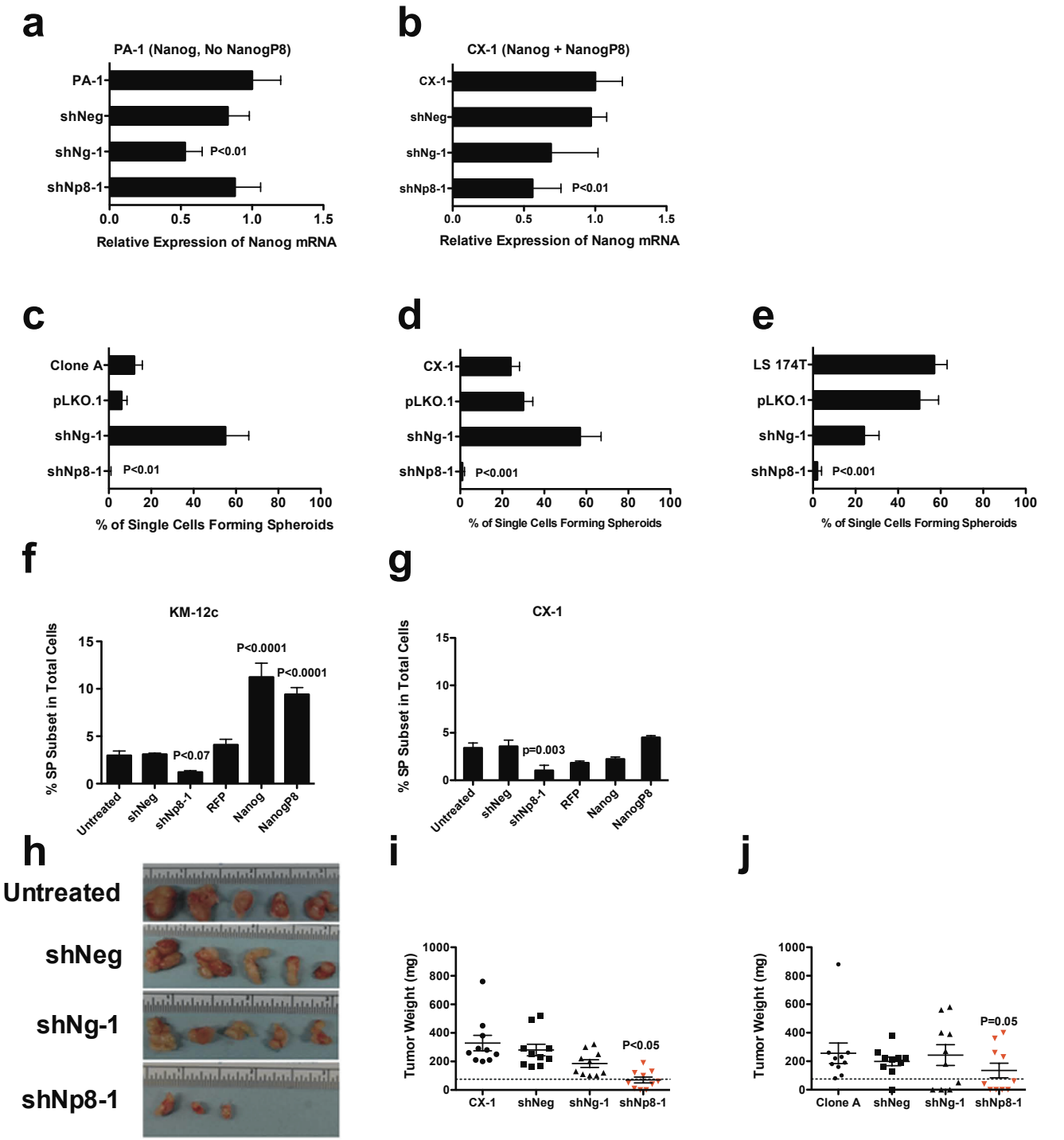
a
PA-1 (Nanog, No NanogP8)
PA-1
shNeg
shNg-1
shNp8-1
P<0.01
0.0
0.5
1.0
1.5
Relative Expression of Nanog mRNA
b
CX-1 (Nanog + NanogP8)
CX-1
shNeg
shNg-1
shNp8-1
P<0.01
0.0
0.5
1.0
1.5
Relative Expression of Nanog mRNA
c
Clone A
pLKO.1
shNg-1
shNp8-1
P<0.01
0
20
40
60
80
100
% of Single Cells Forming Spheroids
d
CX-1
pLKO.1
shNg-1
shNp8-1
P<0.001
0
20
40
60
80
100
% of Single Cells Forming Spheroids
e
LS 174T
pLKO.1
shNg-1
shNp8-1
P<0.001
0
20
40
60
80
100
% of Single Cells Forming Spheroids
f
KM-12c
% SP Subset in Total Cells
0
5
10
15
P<0.0001
P<0.0001
P<0.07
Untreated
shNeg
shNp8-1
RFP
Nanog
NanogP8
g
CX-1
% SP Subset in Total Cells
0
5
10
15
p=0.003
Untreated
shNeg
shNp8-1
RFP
Nanog
NanogP8
h
Untreated
shNeg
shNg-1
shNp8-1
i
Tumor Weight (mg)
0
200
400
600
800
1000
P<0.05
CX-1
shNeg
shNg-1
shNp8-1
j
Tumor Weight (mg)
0
200
400
600
800
1000
P=0.05
Clone A
shNeg
shNg-1
shNp8-1

Figure 6.

Supplementary Materials

7 Figures

1 Table

Supplementary Figure Legends

Supplementary Figure 1 Nanog Peptides can block the Nanog staining in CRC Clinical Samples

(a-b) 5 μ formalin-fixed paraffin embedded specimens of liver metastases sections were analyzed for the expression of Nanog protein (green) and Nanog antibody was blocked with synthetic Nanog peptides. Antibodies were a final dilution of 1:100. Patient 2 is shown. When the antibody to Nanog was blocked with synthetic Nanog peptides, the fluorescence due to Nanog was removed (b). Images were captured on a Nikon 90i microscope with a DU888 EMCCD camera and analyzed with NIS-Elements software. Object magnification, 20X. White bar 10 microns.

(c-e) Polyclonal goat anti-Nanog (R&D Cat No. AF1997(c), Mouse Monoclonal Anti-Nanog (Cell Signalling Cat No. , 4893 (d) and rabbit Monoclonal Antibody (Cell Signalling Cat No. 4903 (e) were incubated with 3 synthetic peptides (2 22mers 5' to the the homeobox domain of Nanog and 1 21mer 3' to that domain) in 0.15 M PBS overnight at 4°C. These blocked antibodies were then assessed and compared to unblocked antibody for reactivity on western blots prepared as described in Materials and Methods. Final dilutions of unblocked (UB) and blocked (B) antibodies were 1:500 (c-e). Lysates of both Clone A and CX-1 were probed in Panel A and CX-1 alone in Panels B and C. Arrowheads indicate expected mass of NANOG in each blot.

Supplementary Figure 2. Expression of stem cell-related membrane antigen genes are not Upregulated in Spheroids in CRC

(a-b) Total RNA was extracted and qRT-PCR was performed for CD44, CD133 and CD166. The results were normalized to GAPDH and HCC 2998 monolayers. Mean % ± SD.

Supplementary Figure 3 Sequence Alignment of Human Nanog and Deduced NanogP8 Protein and Allele Specific shNP8-1.

(a) The deduced NanogP8 protein was aligned with Nanog with the 2 – not just the 1 – different amino acids highlighted by the: and red underline.

(b) Allele-specific silencing of NanogP8, shNP8-1 was designed with the SNP aligned with position 10 of the guide strand according to Huang *et al* (Huang *et al*., 2009) and Dyxhoorn *et al* (Dyxhoorn *et al*., 2006).

Supplementary Figure 4 shRNA to Nanog reduces expression of Oct4 and SOX2

(a-b) shRNA to Nanog decreases Oct4 and SOX2 transcripts in CRC;

(c-d) Secondary transduction of either Nanog or NanogP8 into CloneA and CX-1 transduced previously with shNanog increases Nanog or NanogP8 expression, respectively. P values by contingency table analysis with Bonferroni correction. * P<0.01 shNanog in Clone A and CX-1 vs shNanog+Nanog, shNanog+NanogP8 in Clone A and CX-1, respectively. Mean % ± SD.

Supplementary Figure 5 Nanog is Expressed in PA-1 cells and TFs expression in SP of CX-1

(a) Restriction endonuclease digestion of 260 nt length of Nanog by RT-PCR amplified from PA-1 cells which demonstrates that only Nanog is present in PA-1 cells. Nanog and NanogP8 are two controls. (b) Expression of *NANOG*, *OCT4* and *SOX2* was analyzed in CX-1, CX-1 SP and non-SP cells by qRT-PCR. P values by contingency table analysis with Bonferroni correction. * P<0.01 vs Parental CX-1.

Supplementary Figure 6 Side Population Analyses of KM-12c Transduced with shNeg and shNp8-1.

KM-12c cells were transduced with LVs containing shNeg, shNP8-1 (shNanogP8-1) or not transduced and then analyzed for the side population as described in the text.

Supplementary Figure 7 Side Population Analyses of KM-12c Transduced with RFP, NanogP8 or Nanog. Km-12c cells were transduced with Red Fluorescent Protein (RFP), *NANOG* or *NANOGP8* and then analyzed for the side population as described in the text.

KM-12c cells were transduced with RFP alone, NanogP8 or Nanog and then subjected to analysis of the side population. The results of Supplementary Figures 6-7 are graphically displayed in Figure 5.

Supplementary Table

Table 1. Nanog and NanogP8 Transcripts in Deidentified Patients Whose CRC Liver Metastases Were Resected at the NIH Clinical Center

		Gene Transcript				
Patient		Normal		Tumor		
Number	Gender	Nanog	NanogP8	Nanog	NanogP8	IFA
1	F	-	-	+	-	+
2	M	-	-	-	-	+
3	M	+	-	+	+	+
4	F	-	-	+*	-	-
5	M	+	+	+	+	+
6	F	+	-	+	+	+
7	M	+	-	+	+	+
8	F	-	-	+	+	+
9	F	-	-	+	+	+
10	F	-	-	-	-	-
	6F/4M	4/10	1/10	8/10	6/10	8/10

Legend: all patients are de-identified with the only characteristic known by authors is gender (F- Female, M-Male). No other pathologic or demographic characteristics are known except that patients all have stage IV CRC with liver metastases that were resected at the NIH Clinical Center. Nanog or NanogP8 transcripts were identified as described by RT-PCR and the ALwNI endonuclease assay. Eight of 10 metastases express NanogP8, Nanog or both. IFA was performed as described in Materials and methods.

*Tumor from Patient 4 has weak expression on the total Nanog gel of a Nanog transcript (Figure 1) but was not assessable by AlwNI endonuclease digestion or Sanger sequencing so that a Nanog family member is present but it is not clear whether it is Nanog or NanogP8.

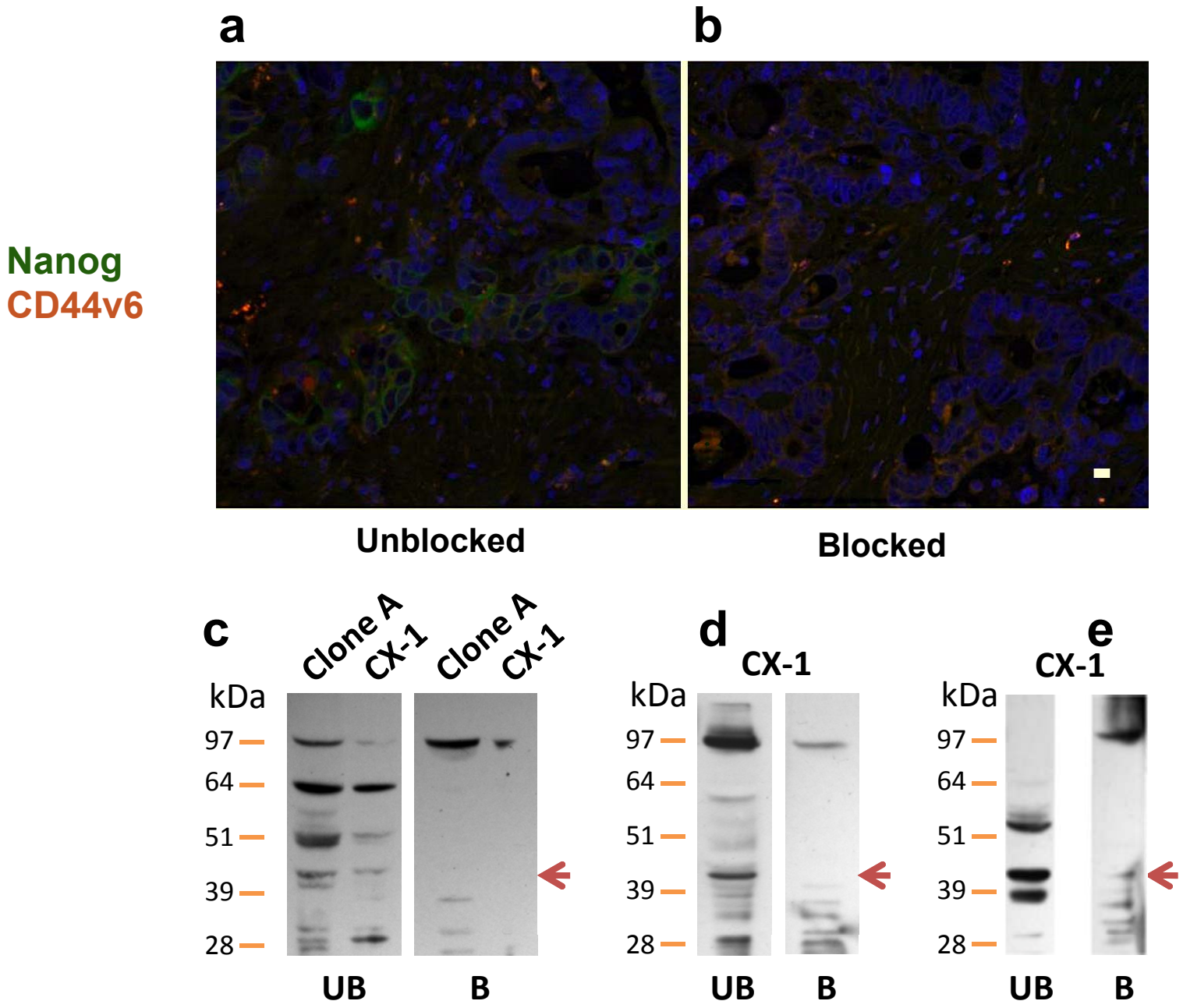

Supplementary Figure 1

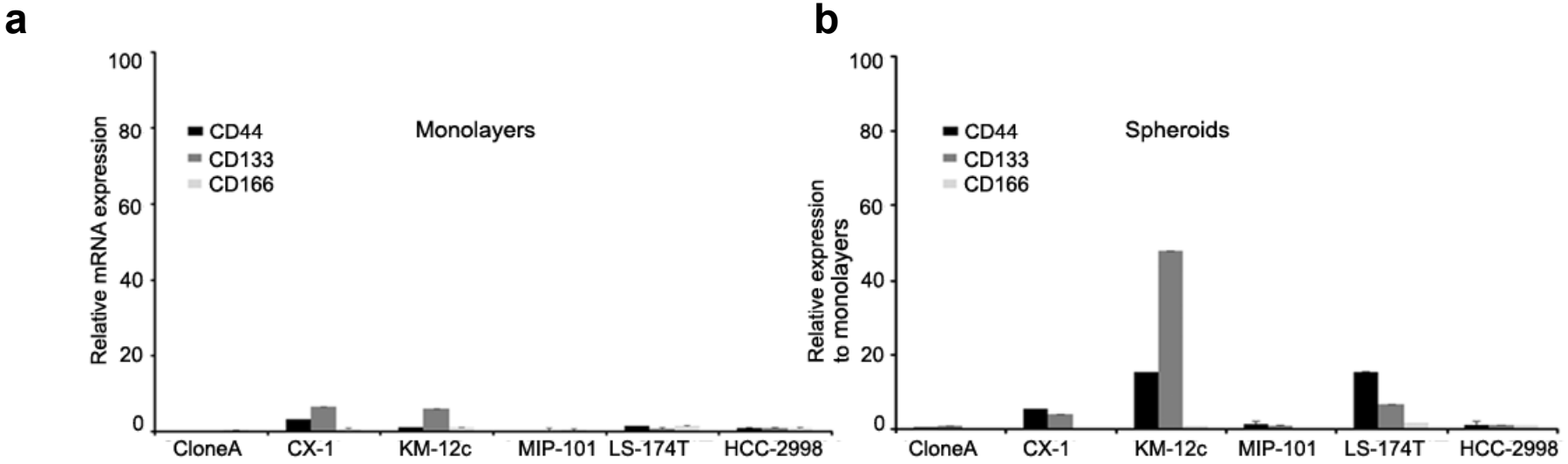

Supplementary Figure 2

a

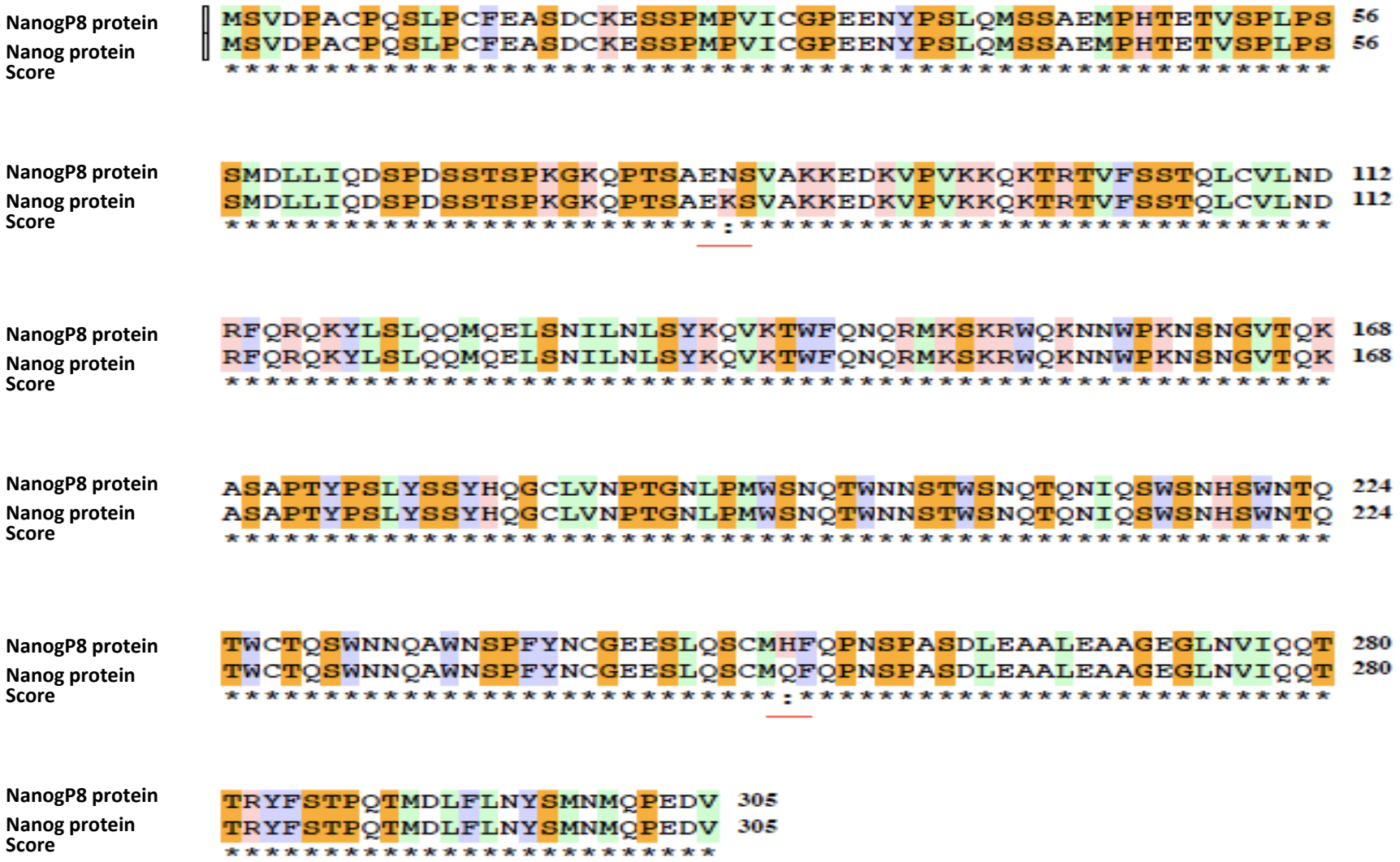

b

NANOGP8 5’—-AATCTCTGCAGTCCTGCATGCA**C**TTCCAGCCAAATTCTCCTGCC—3’

siRNA shNP8-1a 5’-CUGCAUGCA**C**UUCCAGCCA-3’

shNP8-1b 5’-UGGCUGGAAGUGCAUGCAG-3’

Supplementary Figure 3

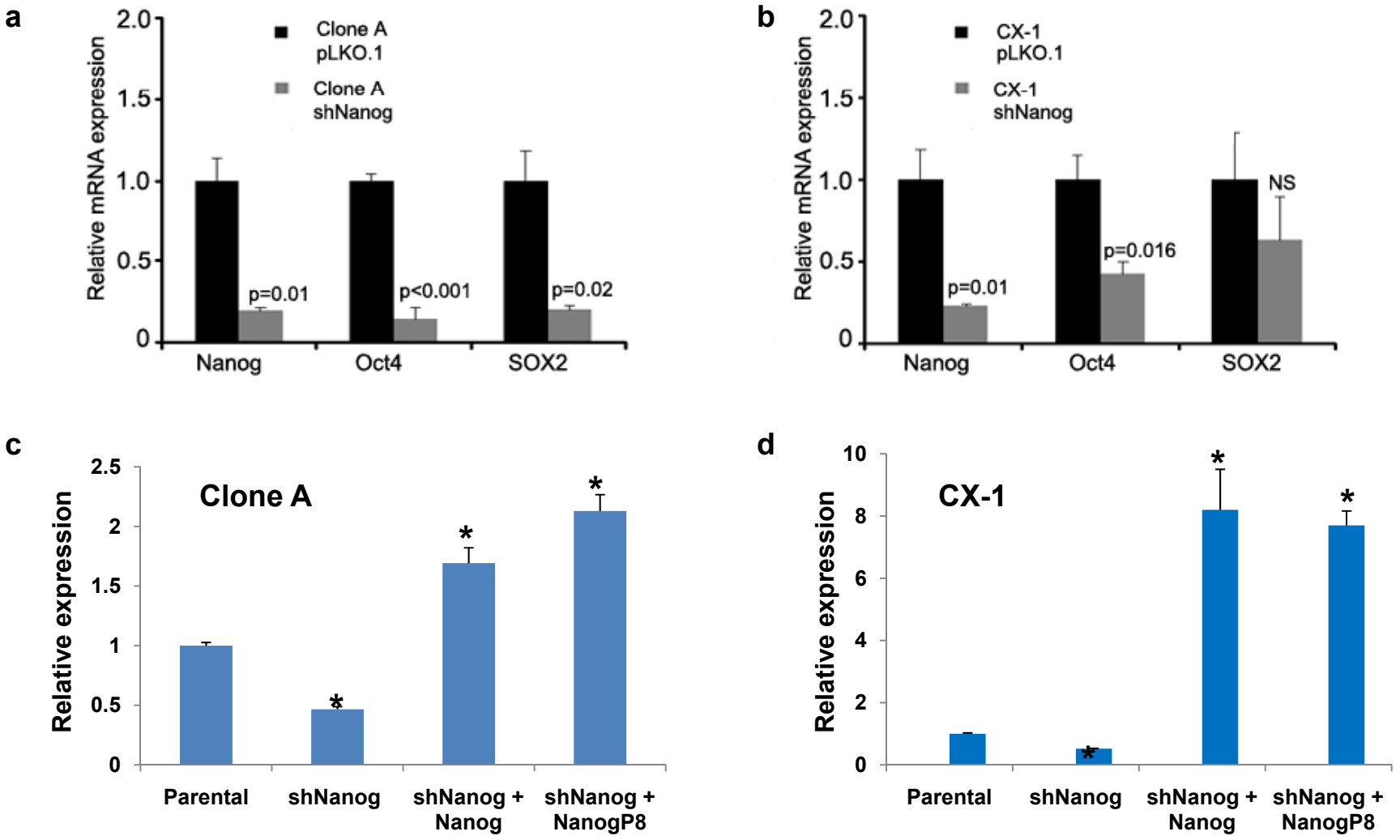

Supplementary Figure 4

a

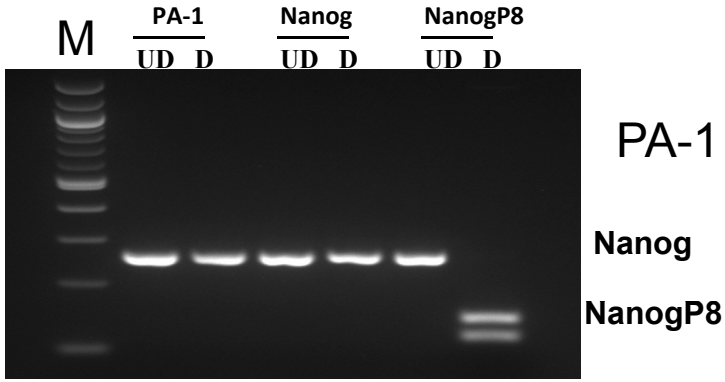

b

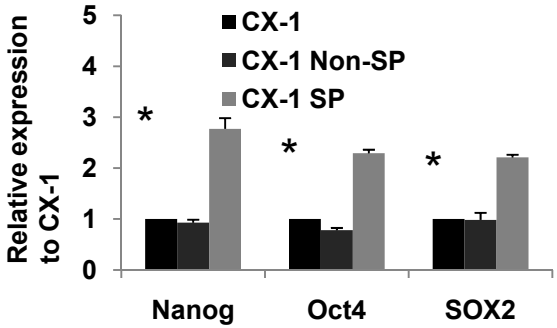

Supplementary Figure 5

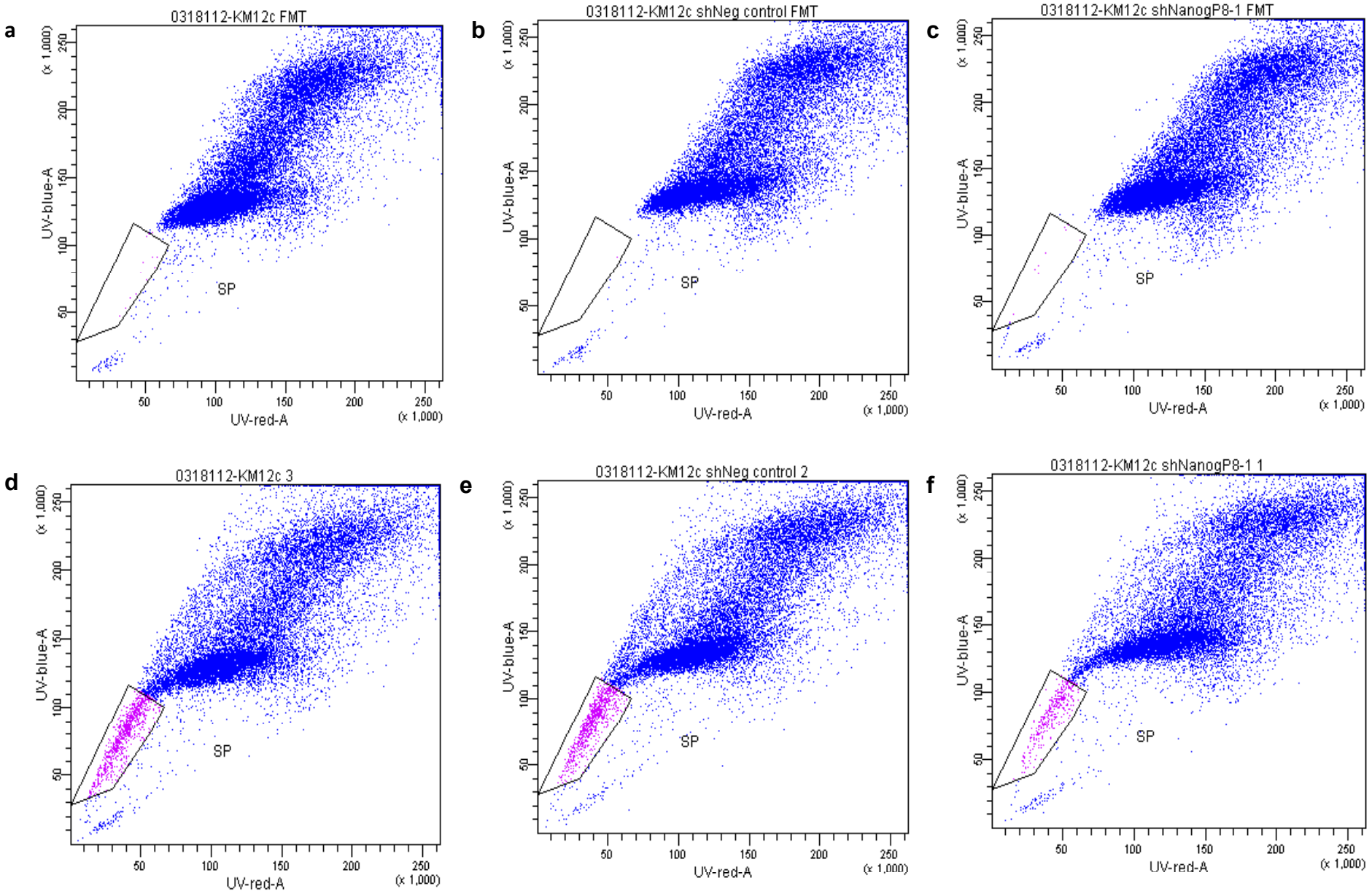

Supplementary Figure 6

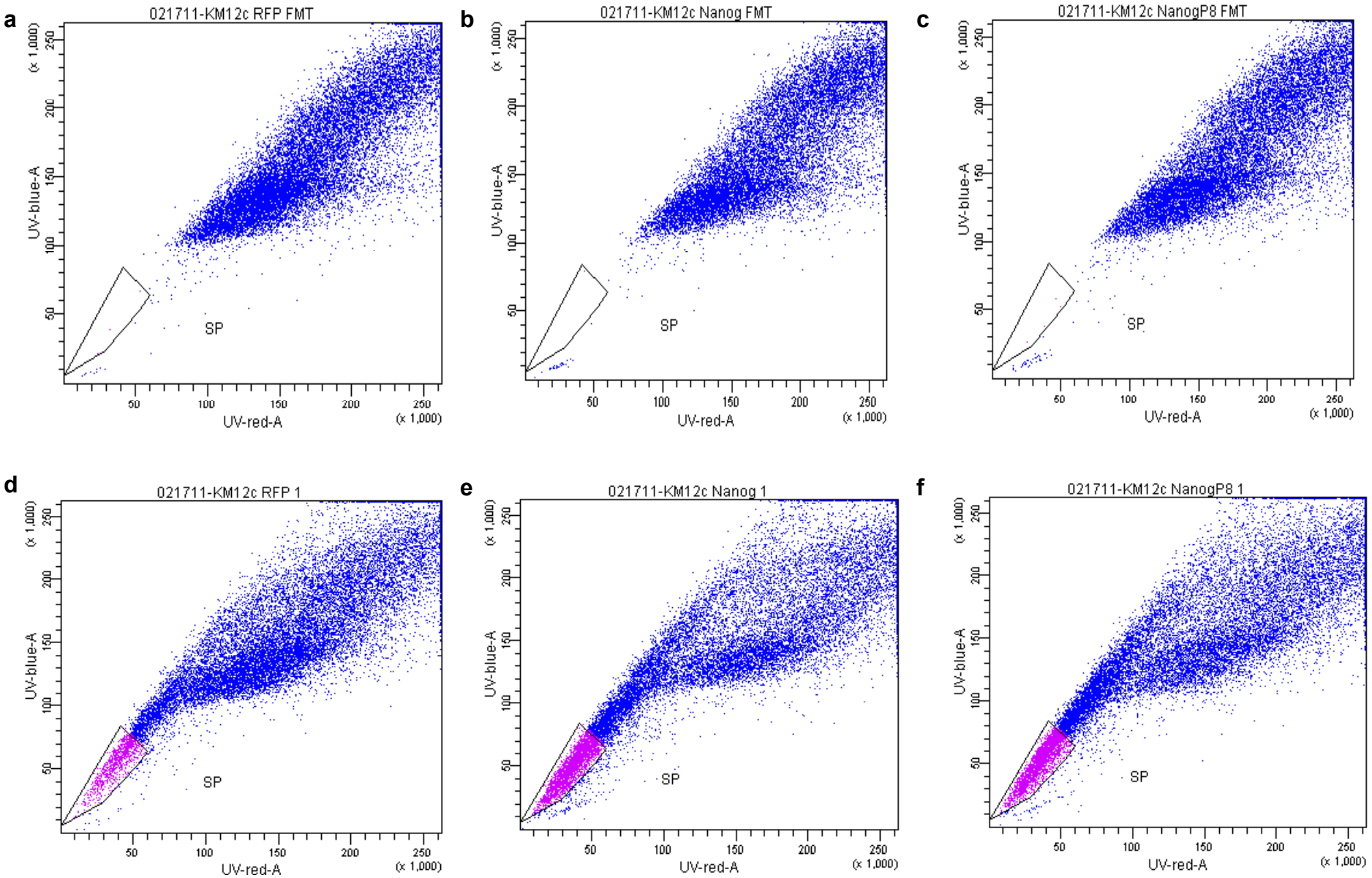

Supplementary Figure 7

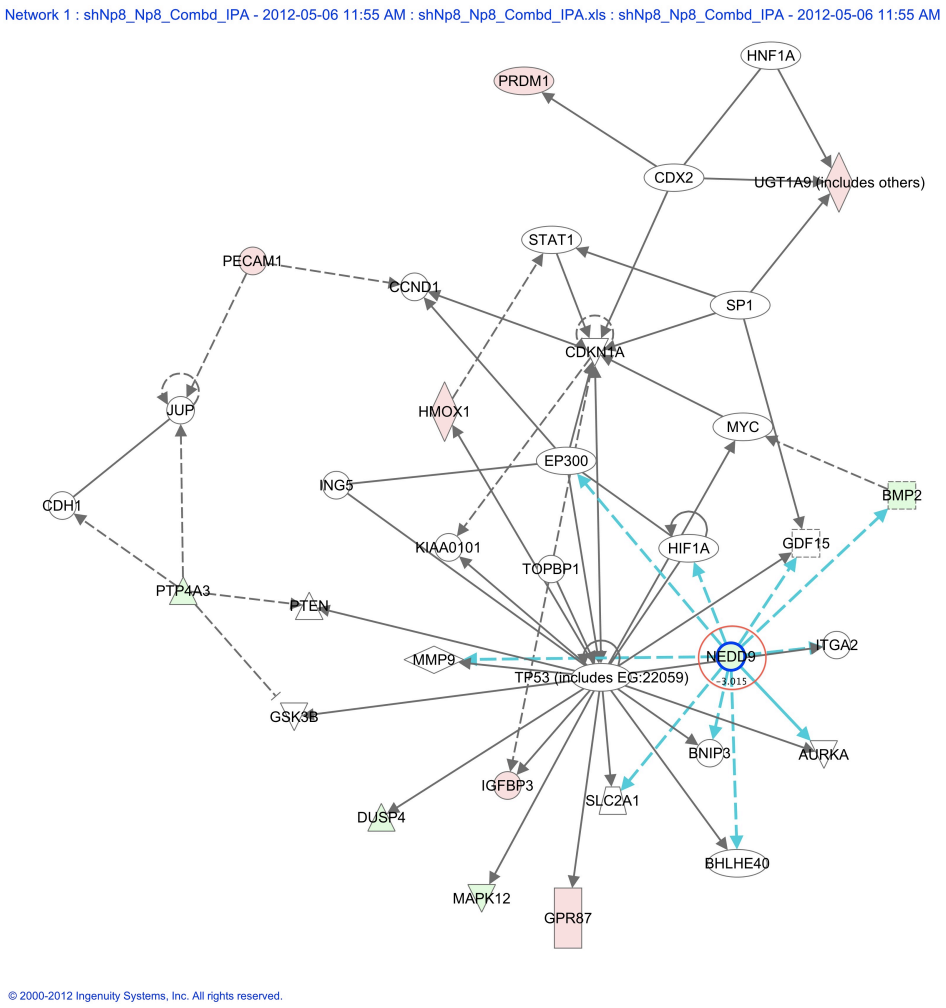

Figure 1. NANOG regulates NEDD9 and other genes. CX-1 cells in monolayer were transduced for 7 days with LV shNp8-1 or LV NANOGP8 to modulate genes controlled by NANOG. RNA was isolated and subjected to RNA-Seq on an Illumina IIgX platform after library construction according to the manufacturer's protocol. The genes that were significantly discordantly expressed (Up-Down or Down-Up for shNp8-1 vs NANOGP8 overexpression) were subjected to IPA analysis and graphed here. NEDD9 was significantly downregulated (red circle) by shNp8-1 along with several other genes that were previously known to be differentially regulated in embryonic stem cells (eg, BMP2).

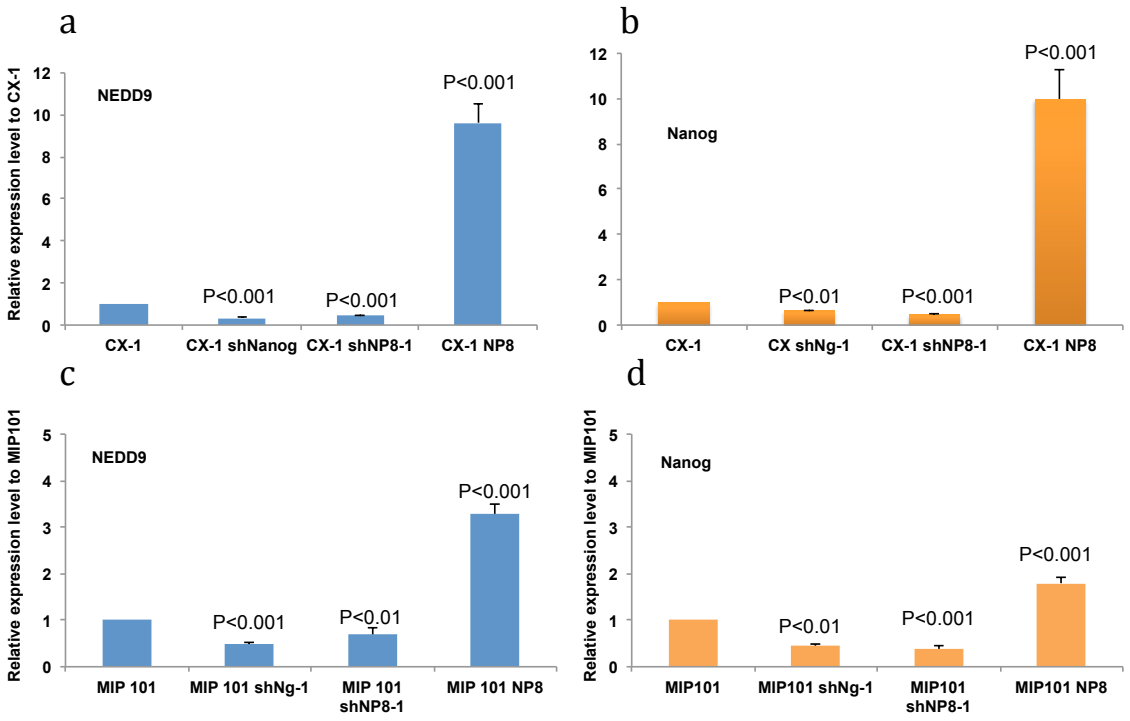

Figure 2. Modulation of Nanog Gene Expression Directly Affects NEDD9 Transcript Levels. CX-1 or MIP-101 human CRC cells were transduced with LV shNp8-1 or shNg-1 to inhibit NANOGP8 or NANOG, respectively or with LV NANOGP8 (NP8) to increase NANOG expression for 3 days before RNA was harvested and qRT-PCR performed for NANOG and NEDD9 transcripts. shNp8-1 significantly decreases and NP8 increases NANOG transcript levels in CX-1 (Panel b) and MIP-101 (Panel d) cells. These changes in NANOG transcripts are associated with parallel changes in NEDD9 transcript levels (Panels a and b). Inhibition of NANOG by either shNg-1 in MIP-101 (Panel c) or shNanog in CX-1 (Panel a) also decreased NEDD9 levels. Results are mean ± SD of results normalized with GAPDH. P values are compared to the untreated control cells by one way ANOVA with a TUKEY post-test for multiple comparisons.

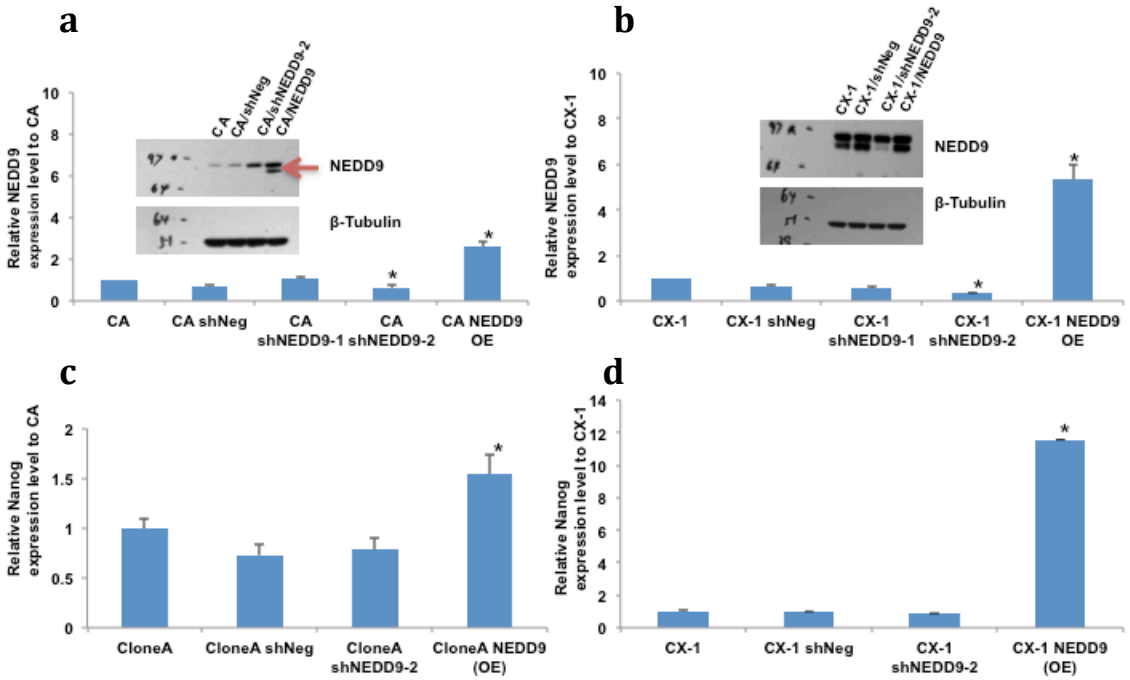

Figure 3. Effect of shRNA to NEDD9 on Transcript and Protein Overexpression. Clone A (CA) or CX-1 CRC cells were cultured for 4 days in monolayer with LV containing shRNA to NEDD9 (shNEDD9-1 or shNEDD9-2) or NEDD9 to overexpress (OE) the protein. Cells were harvested and qRT-PCR and western blots (insets) were performed. Panels (a, b) are relative expression of gene transcripts of NEDD9 and Panels (c, d) are NANOG transcripts. LV delivered shNEDD9-2 inhibits NEDD9 transcription (Panels a, c) but reduced NEDD9 protein only in CX-1 (Panel b) and then only the lower of the 2 bands of NEDD9 protein recognized on western blots (Other investigators have shown that the upper band is heavily phosphorylated whereas the lower band has less phosphorylation). Interestingly, overexpression of NEDD9 increased NANOG transcripts (Panels c,d) which suggests that NEDD9 can stimulate NANOG transcription. shNEDD9-2 did not inhibit expression of NEDD9 compared to untreated cells (Panel a). Results are mean ± SD. * is $P < 0.01$ versus untreated CRC cells.

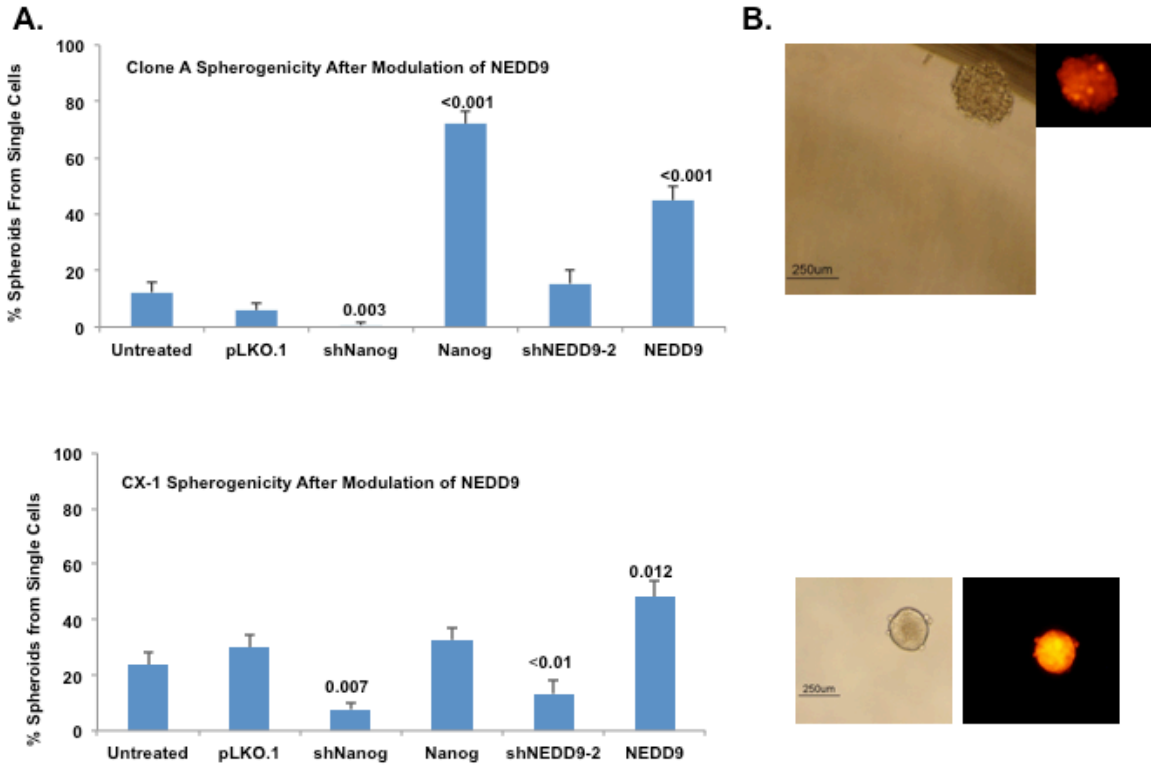

Figure 4. Modulation of NEDD9 Expression Directly Affects Single Cell Spherogenicity. CX-1 or Clone A (CA) cells were transduced with the indicated LV construct. In Panel A the mean ± SD of the percentage of single cells that formed spheroids of 50 or more cells is indicated. P values in Panel A are compared to the Untreated cells with Bonferroni correction for multiple comparisons. Panel B indicates that spheroids form cells transduced with NEDD9 for overexpression express red fluorescent protein (RFP) that was the reporter in the LV used for overexpression.

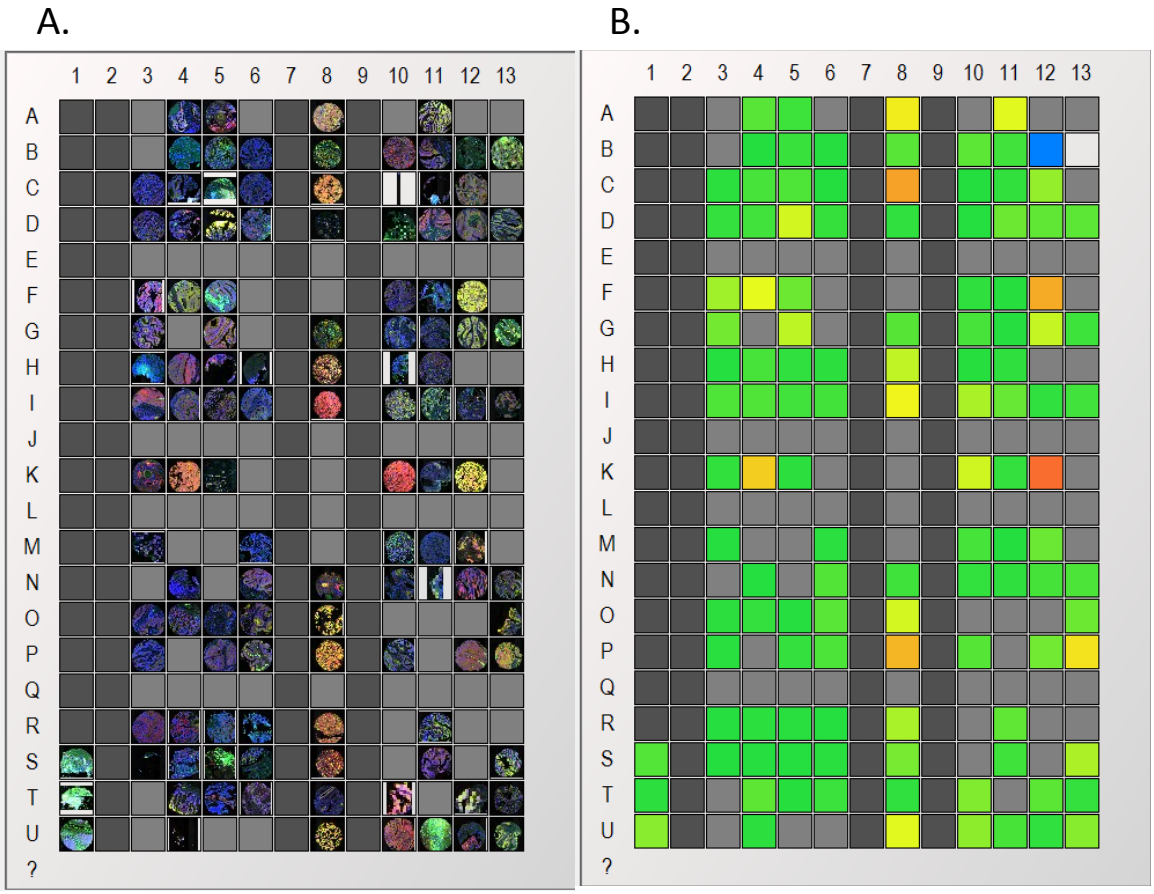

Figure 5. qIFA of Slide 1 of the Colon Carcinoma TMA. The first of 4 slides that comprise the Cancer Diagnosis Program's Colon Cancer Prognostic Array. The slide has been stained with primary antibodies for CD44v6 (Red) and NANOG (Green). Nuclei are counterstained with DAPI (Blue) and scanned with an Aperio Fluorescence Scanscope (Panel A). The image has been then analyzed with the Definiens Tissue Studio analysis program and a heat map created of Panel A for NANOG intensity based from low (Green) thru Medium (Yellow) to High (Red).

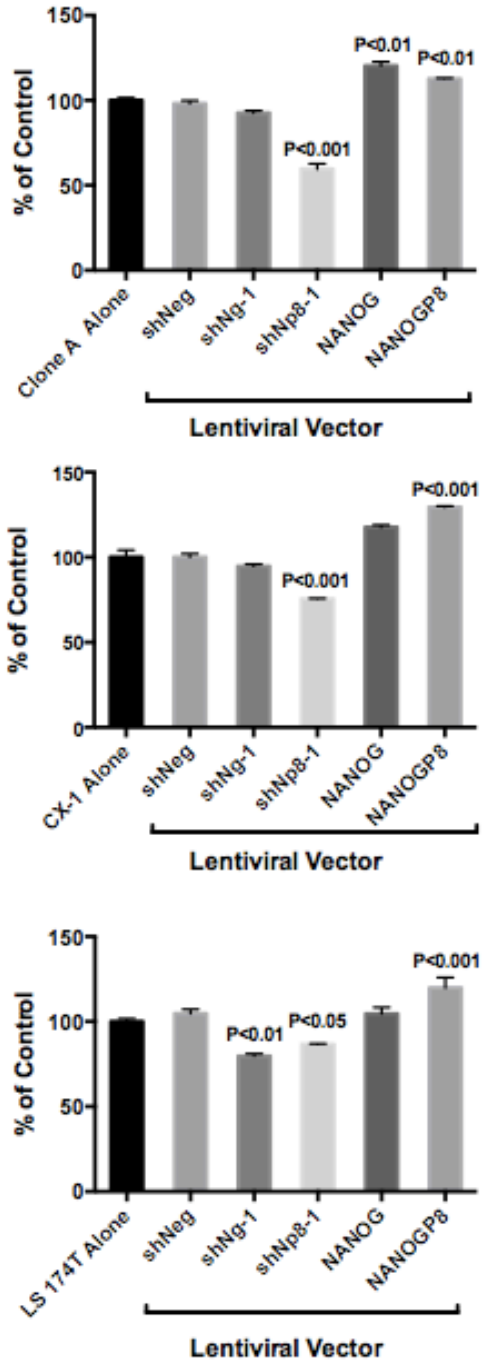

Figure 6. Proliferation by LV shRNA and Overexpression of NANOG and NANOGP8. Clone A, CX-1 or LS 174T cells were transduced with vectors indicated and cultured for 3 days in monolayer and then proliferation assessed by WST1 and Absorbance measured on a plate reader at 405 nm. Results are mean ± SD normalized by the cells alone control. P values are compared to cells alone control with Bonferroni correction for multiple comparisons. The LV shRNA to NANOGP8 (shNp8-1) consistently inhibits proliferation whereas overexpression of NANOGP8 stimulates proliferation.

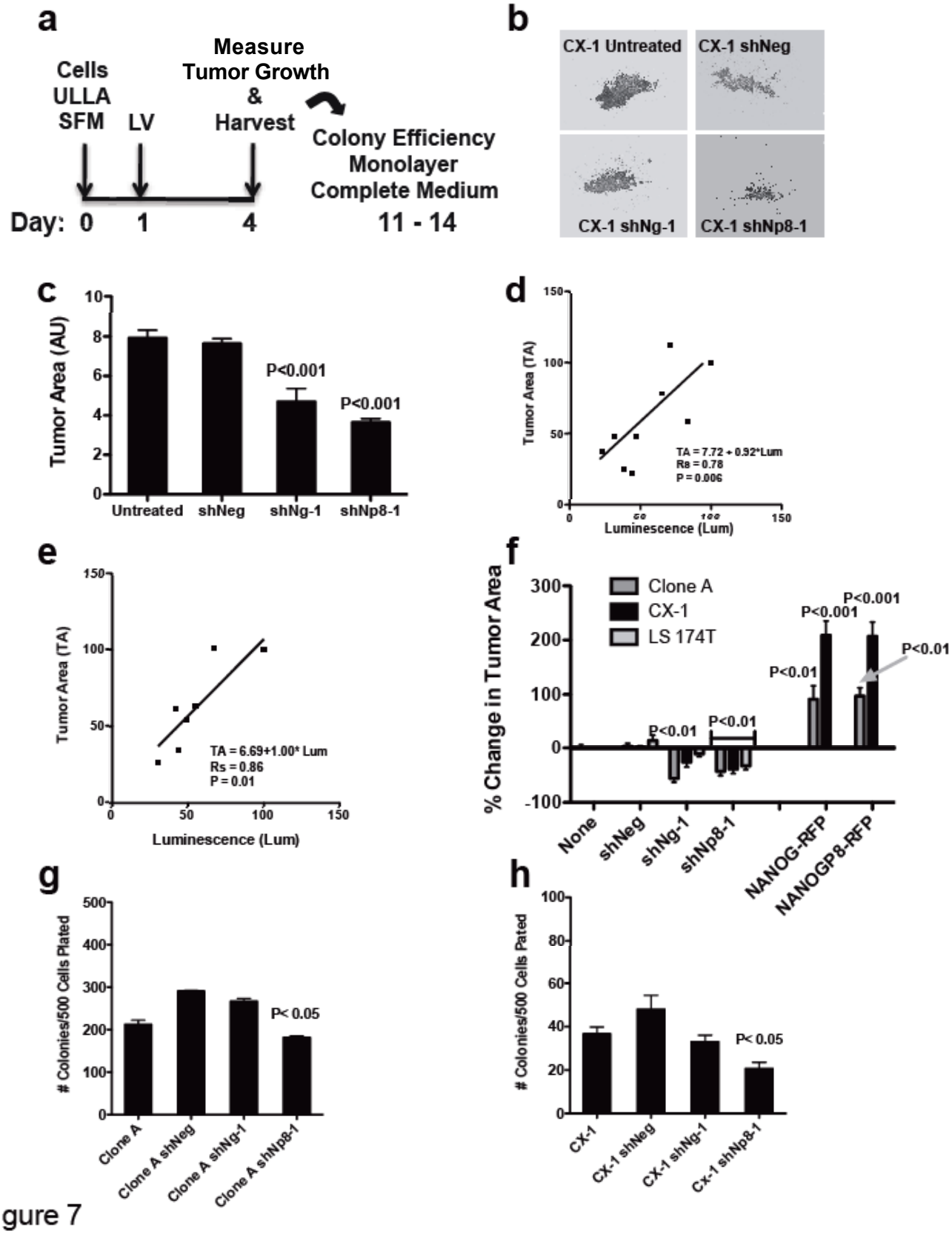
a
Cells
ULLA
SFM
LV
Measure
Tumor Growth
&
Harvest
Colony Efficiency
Monolayer
Complete Medium
Day: 0 1 4
11 - 14
b
CX-1 Untreated
CX-1 shNeg
CX-1 shNg-1
CX-1 shNp8-1
c
Tumor Area (AU)
P<0.001
P<0.001
Untreated
shNeg
shNg-1
shNp8-1
d
Tumor Area (TA)
TA = 7.72 + 0.92*Lum
Rs = 0.78
P = 0.006
Luminescence (Lum)
e
Tumor Area (TA)
TA = 6.69+1.00* Lum
Rs = 0.86
P = 0.01
Luminescence (Lum)
f
% Change in Tumor Area
Clone A
CX-1
LS 174T
P<0.01
P<0.01
P<0.01
P<0.001
P<0.001
None
shNeg
shNg-1
shNp8-1
NANOG-RFP
NANOGP8-RFP
g
Colonies/500 Cells Plated
P< 0.05
Clone A
Clone A shNeg
Clone A shNg-1
Clone A shNp8-1
h
Colonies/500 Cells Pated
P< 0.05
CX-1
CX-1 shNeg
CX-1 shNg-1
Cx-1 shNp8-1

Figure 7

Figure 7. Lentiviral shRNA Treatment of CRC Cells in Suspension Inhibits Tumor Growth. (a) the protocol for treatment of CRC: cells stably transfected with *Luc2* were plated overnight in serum-free medium in ULLA plates and then exposed to lentiviral particles at a MOI of 5-16:1. Three days later cultures were analyzed by luminescence, low power microscopy with an inverted Nikon microscope or by confocal microscopy. Surviving cells were harvested and then plated in complete medium in standard culture medium to assess the potential for regrowth after transduction with shRNA. (b) A typical result of exposure to either shNg-1, shNp8-1 or the control shNeg 72 hr after transduction in suspension culture. 2X magnification. (c) Tumor area as measured with ImageJ in arbitrary units. In ULLA plates suspension cultures were contained within the field of view of a 2x objective of the Nikon !8100 inverted microscope. Results (Mean ± SD) of a typical experiment with CX-1 cells presented. (d, e) Correlation across 3 repetitive experiments with CX-1 (d) and 2 experiments with Clone A (e) cells between luminescence and optical measurement of Tumor Area. (f) Summary of 15 experiments with 3 CRC lines treated with lentiviral delivered shRNA as indicated to inhibit tumor growth or with NANOG or NANOGP8 to stimulate growth. All results were normalized to the untreated control within each experiment and then the Means ±SD of repetitive experiments presented. (g, h) Cells that survived the original 72 hr of exposure were harvested and replated in complete medium in 10 cm Petri dishes and Mean ± SD of the number of colonies formed in Clone A (g) or CX-1 (h) cells. P values are compared to untreated control cells by one-way ANOVA or contingency table analysis with Bonferroni correction.

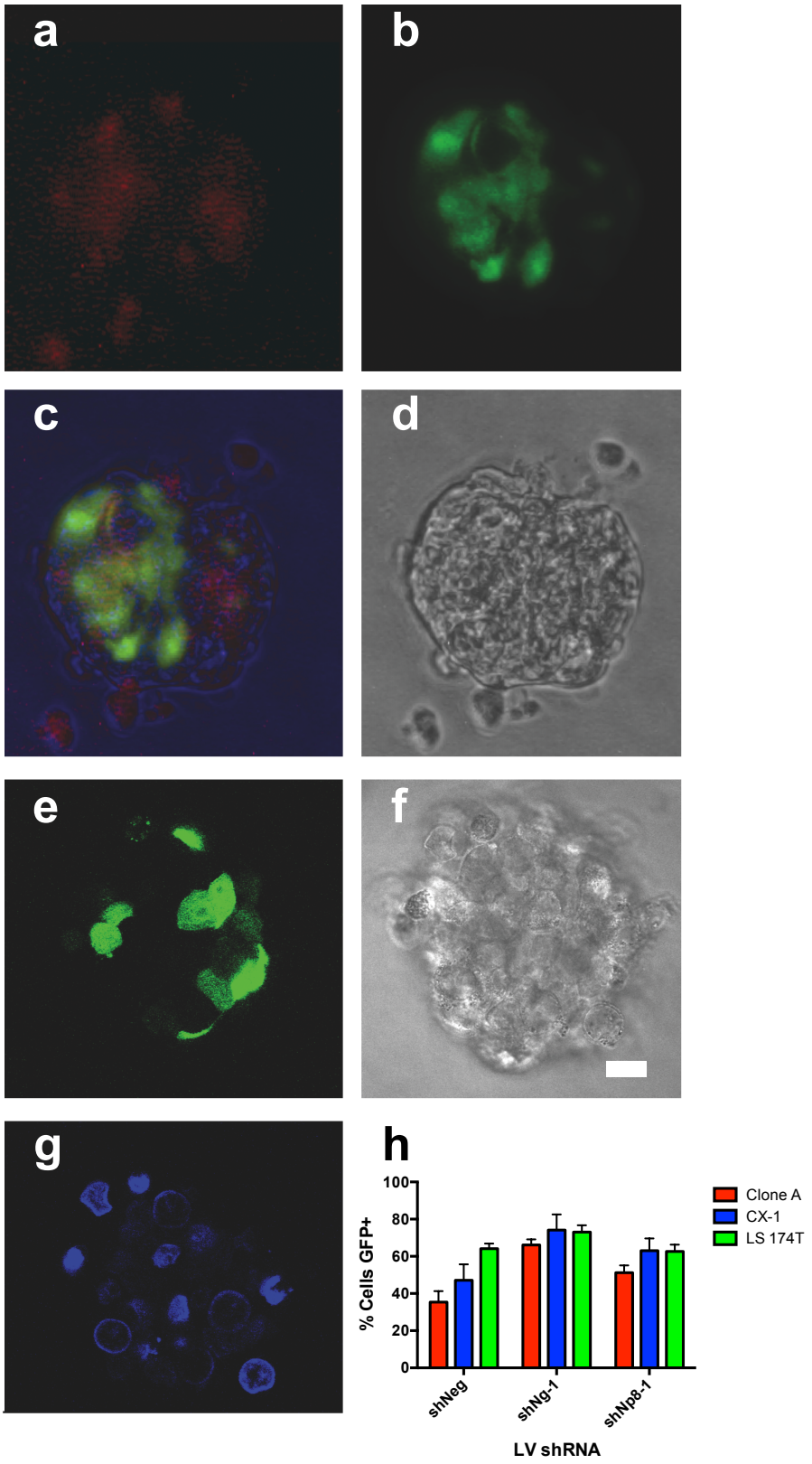
a
b
c
d
e
f
g
h
% Cells GFP+
100
80
60
40
20
0
shNeg
shNg-1
shNp8-1
LV shRNA
Clone A
CX-1
LS 174T

Figure 8

Figure 8. Caspase 3 Activity and Transduction Efficiency of CRC Spheroids. LS 174T (Panels a – d) and CX-1 (e – g) spheroids are imaged by inverted microscopy (a – d) or by confocal microscopy (e – g). Spheroids were incubated with 1 μM PhiPhiLux G_2D_2 for 45 min at 37°C and then imaged for rhodamine fluorescence (a). The same spheroid was then imaged in the fluorescein channel (b), transilluminated (d) and the merged image is shown (c). Spheroids were also subjected to confocal microscopy to assess transduction efficiency in planar sections imaged in the fluorescein channel to detect GFP (e), transilluminated to assess cell location (f), and DAPI-stained nuclei in the UV channel (g). The percentage of cells within each plane of the confocal image that were GFP+/DAPI+ was summed over at least 3 experiments for each cell line (Mean ± SD) in (h).

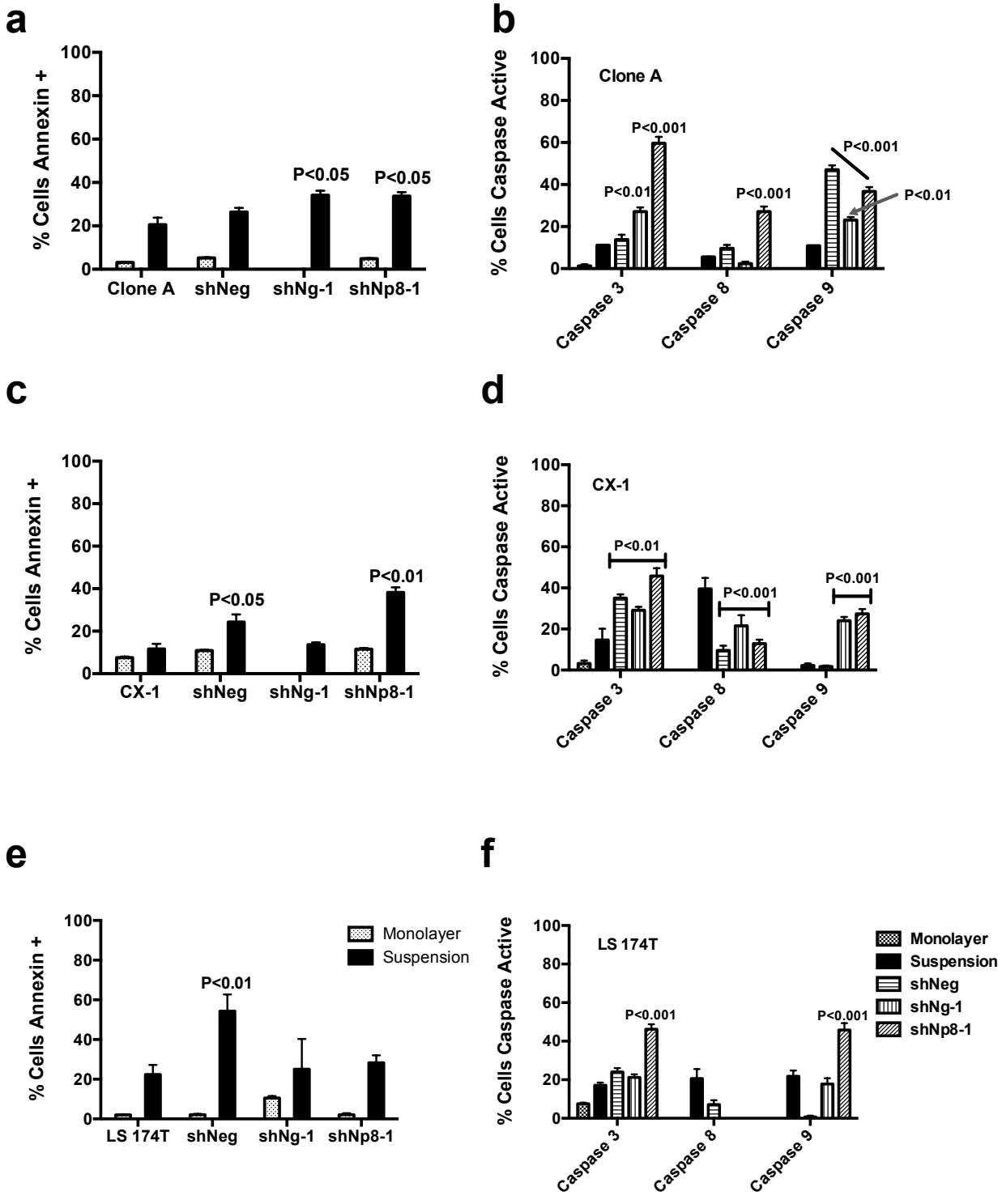
a
% Cells Annexin +
100
80
60
40
20
0
P<0.05
P<0.05
Clone A
shNeg
shNg-1
shNp8-1
b
% Cells Caspase Active
Clone A
P<0.001
P<0.01
P<0.001
P<0.001
P<0.01
Caspase 3
Caspase 8
Caspase 9
c
% Cells Annexin +
P<0.05
P<0.01
CX-1
shNeg
shNg-1
shNp8-1
d
% Cells Caspase Active
CX-1
P<0.01
P<0.001
P<0.001
Caspase 3
Caspase 8
Caspase 9
e
% Cells Annexin +
Monolayer
Suspension
P<0.01
LS 174T
shNeg
shNg-1
shNp8-1
f
% Cells Caspase Active
LS 174T
P<0.001
P<0.001
Monolayer
Suspension
shNeg
shNg-1
shNp8-1
Caspase 3
Caspase 8
Caspase 9

Figure 9

Figure 9. Single Cell Profiling of Annexin and Caspase Activity. Clone A (a, b), CX-1 (c, d) or LS 174T (e, f) cells were incubated with Annxin V-rhodamine (a, c, e) or 10μM of fluorogenic substrate for Caspases 3, 8 or 9 (b, d, f) and caspase activity imaged as described for Caspase 3 in Figure 8. In panels a, c, e monolayer cultures (stippled gray columns) have lower levels of Annexin binding than cells in suspension for 4 days (Black Columns). Lentiviral transduction with shNp8-1 consistently increases Annexin binding in suspension cultures of Clone A (a) or CX-1 (c). P values are compared to the untreated cells in suspension culture.

Caspase 3, 8 and 9 activity was measured in Panels b, d, f for Clone A, CX-1 and LS 174T respectively. Caspase activity was assessed 3 days after transduction with shNeg (▤), shNg-1 (▥)or shNp8-1 (▨). Untreated cells (■) in panels b, d, f represent the parent cell line that is not exposed to any lentiviral vector but growing in suspension. Columns are means ± SD and the P values are compared to the untreated cells in suspension alone. Lentiviral transduction with shNp8-1 consistently increases Caspase 9 and 3 activity compared to the untreated cells in each cell line. shNg-1 treatment is less consistent in its stimulation of Caspase 3 and 9 activity. P values determined by contingency table analysis of triplicate cultures with Bonferroni correction for multiple comparisons.

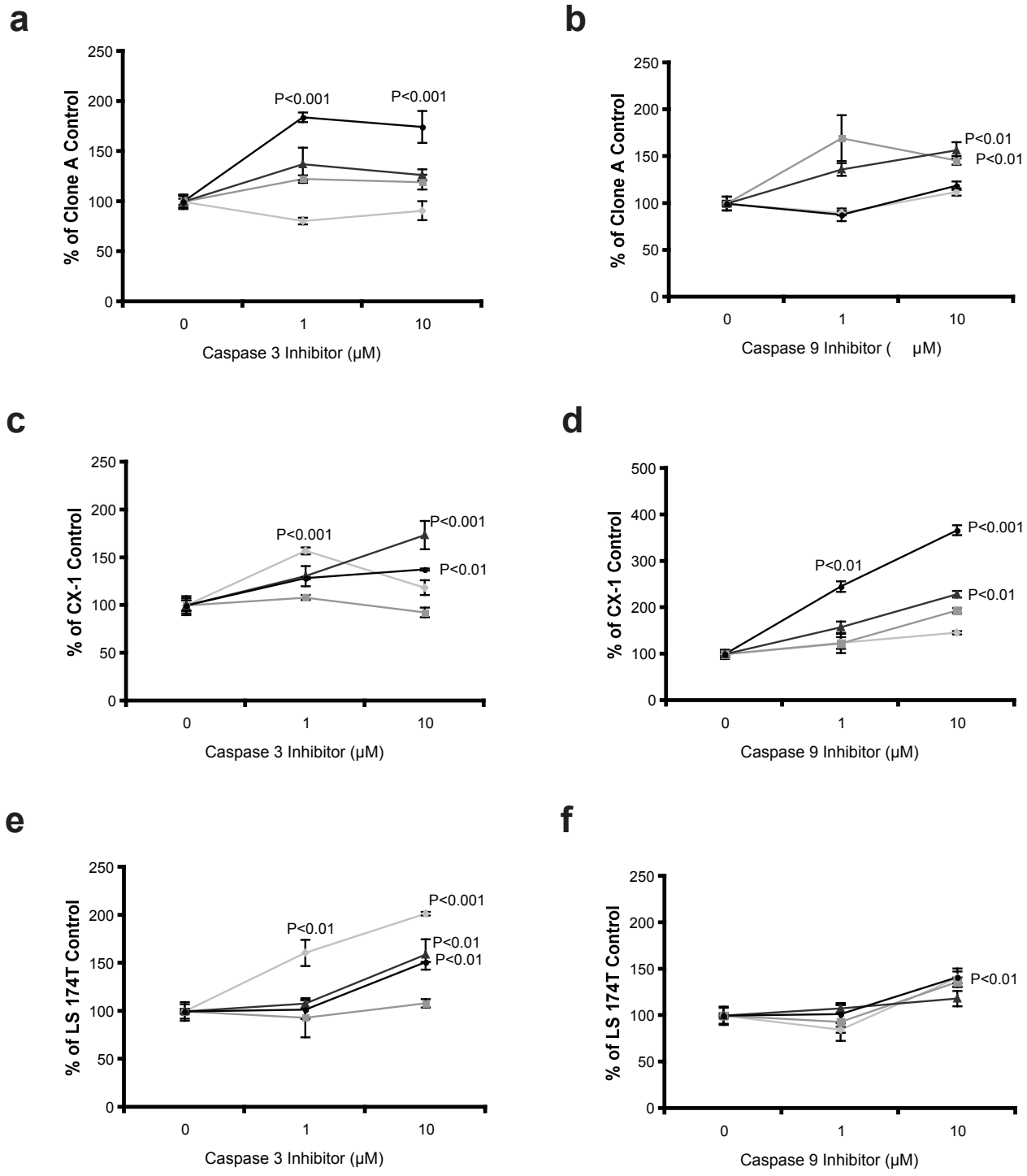
a
% of Clone A Control
P<0.001
P<0.001
Caspase 3 Inhibitor (μM)
b
% of Clone A Control
P<0.01
P<0.01
Caspase 9 Inhibitor (μM)
c
% of CX-1 Control
P<0.001
P<0.001
P<0.01
Caspase 3 Inhibitor (μM)
d
% of CX-1 Control
P<0.001
P<0.01
P<0.01
Caspase 9 Inhibitor (μM)
e
% of LS 174T Control
P<0.001
P<0.01
P<0.01
P<0.01
Caspase 3 Inhibitor (μM)
f
% of LS 174T Control
P<0.01
Caspase 9 Inhibitor (μM)

Figure 10

Figure 10. Inhibition of the Intrinsic Pathway of Apoptosis Blocks the Effect of Lentiviral shRNA to NANOGP8 and NANOG. CRC cells were cultured in SFM and transduced with Lentiviral shNeg (■), shNg-1 (▲), shNp8-1 (●) or left untreated (◆). An hour after transduction, peptide inhibitors for Caspase 3 (Z-DEVD-FMK, Panels a, b, c) or Caspase 9 (Z-LEHD-FMK, Panels d, e, f) were added at the concentrations indicated and suspension cultures continued as described in Figure 7. The tumor areas of the Clone A (a ,d), CX-1 (b, e) and LS 174T (c, f) spheroids were then imaged 3 days after transduction and normalized to the areas of the non-transduced controls. Results are mean ± SD of triplicate cultures.

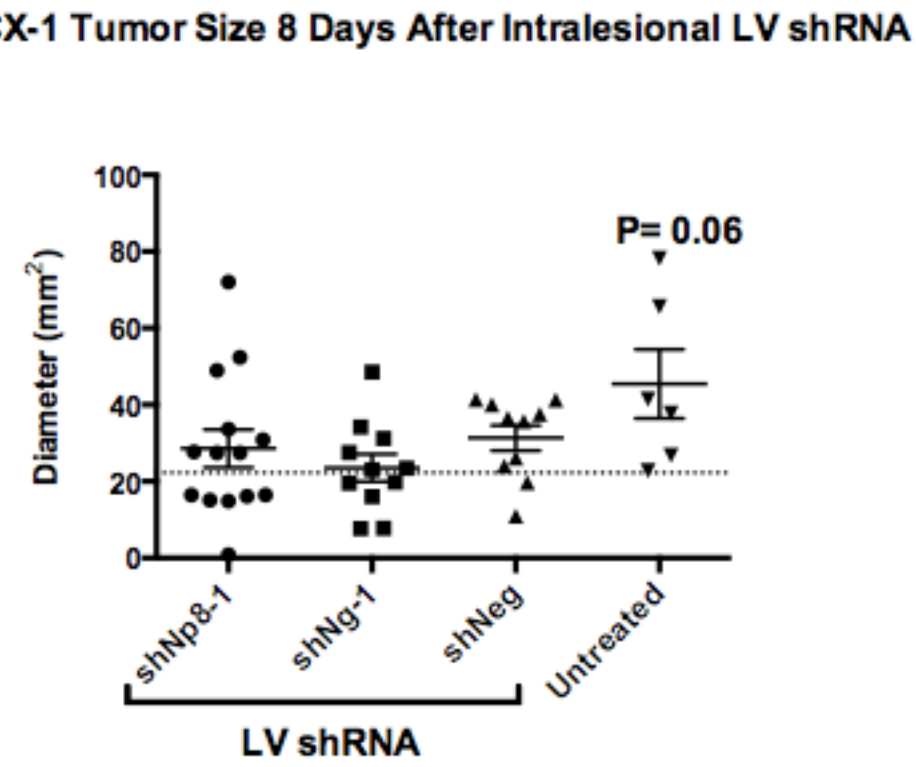

Figure 11. Intralesional LV shRNA Decreases Size of CX-1 subcutaneous nodules. NOD/SCID mice were injected with 1 x 10^6 CX-1 cells subcutaneously in the flank. Nine days later when nodules were 3 – 4 mm diameter they were injected at a MOI of 1 with LV in 0.10 ml PBS with protamine sulfate. Tumor measurements 8 days later are presented with mean ± SD of the area calculated as the product of the two largest perpendicular diameters. There is a trend in favor of the three groups of LV shRNA but it is not significant. When the shNp8-1 and shNg-1 groups are combined and compared to the Untreated and shNeg treated groups, 48% of the two shRNA to NANOGs groups produce tumors smaller than 22.75 mm^2 (the horizontal dashed line) than the 13% of the controls with a $P<0.05$ by Fisher's Exact test.

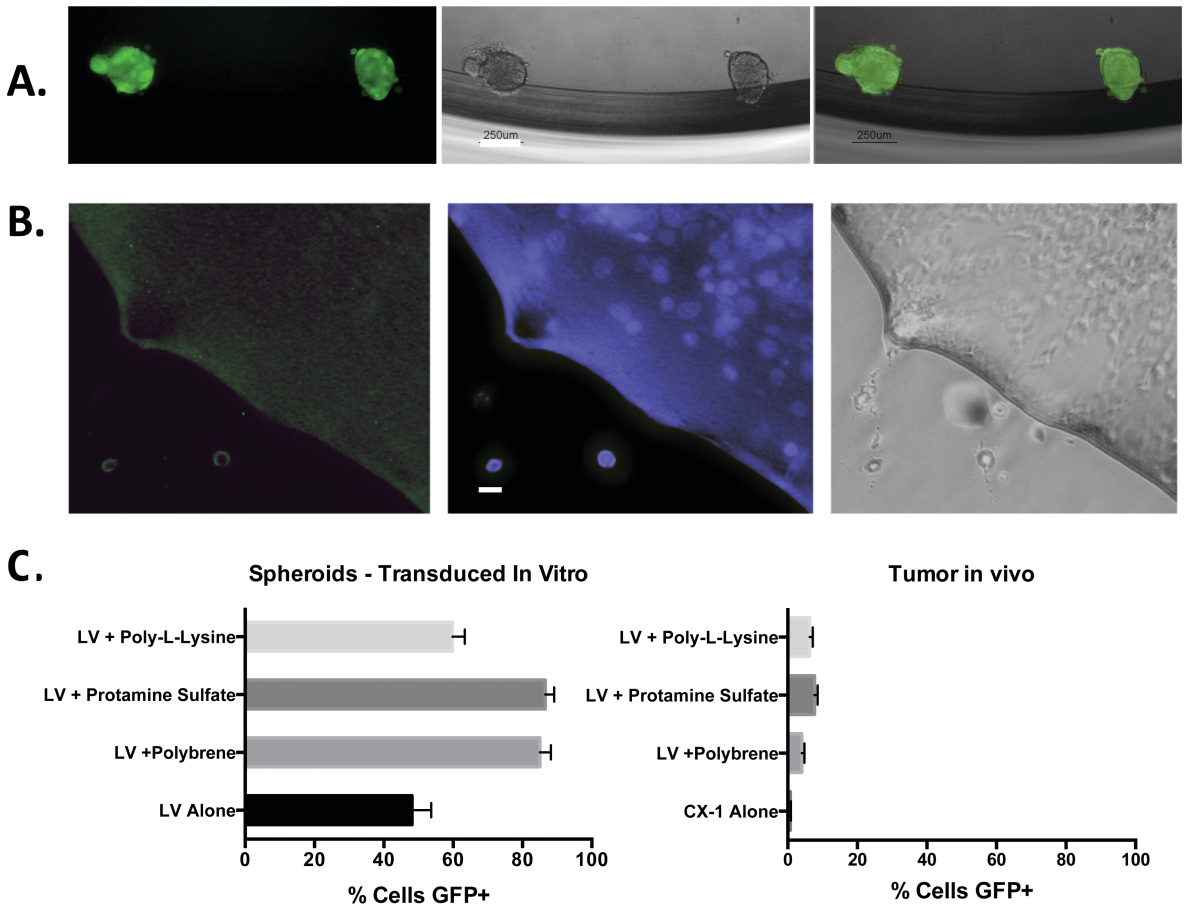

Figure 12. Lentiviral vector mediated shRNA transduces in vitro but minimally in vivo. **Panel A** – CX-1 human CRC cells in suspension transduced after 24 hr in serum free medium at MOI of 5 with LV shNp8-1 and GFP reporter fluorescence imaged at 3 days. Left- GFP Fluorescence under inverted microscope; middle- spheres by transillumination of same field at 4x; Right – Merged image Bar = 250 µ. **Panel B** – 5 mm diameter CX-1 xenografts injected at MOI ~1 with LV shNp8-1 and single cell suspensions made from tumors harvested 5 days later, counterstained with DAPI and imaged at 10x for GFP fluorescence (Left), DAPI (Middle) and transilluminated (Right). Bar – 20 µ. **Panel C** – left panel is per cent of CX-1 cells transduced with LV shNp8-1 from Panel A in the presence of the indicated cations at 8µg/ml imaged 5 days after transduction in vitro while the right panel is for similar transduction after intralesional injection of 3-5 mm diameter CX-1 xenografts 5 days earlier. The cations are adjuvants to improve LV-mediated transduction. There was no GFP+ reporter fluorescence 3 days after intralesional injection of CX-1 xenografts (data not shown).